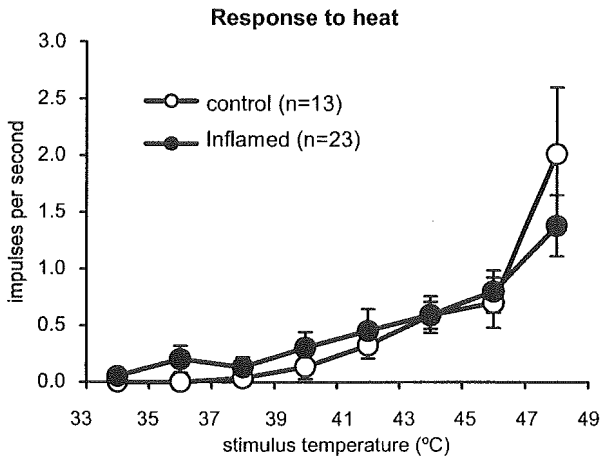

Fig. 8. Stimulus-response curves for C-nociceptors in response to heat stimuli. Open circle: nociceptors from the control rats ($n = 13$), closed circle: those from inflamed rats ($n = 23$). Data are expressed as mean impulses/s ± S.E.M. No significant difference was observed between control and inflamed groups in each temperature sector ($P > 0.05$, Student's t-test).

3.3.4. C-cold units

Location of the receptive field of C-cold units was the same as that of C-nociceptors. Typical C-cold units had spontaneous firing of ~10 Hz (maximum instantaneous frequency: ~85 Hz; Fig. 4, left panel) at 32 °C, and the cutaneous temperature had to be increased up to 35.4 °C (range: 32.1–35.4 °C) to stop this firing. For evaluation of the cold response, 10 out of 12 units in the control group and six out of eight in the inflamed group were used, because the baseline temperature was set to >32 °C in the four units excluded. Four of 10 units in the control group and 2 of 6 in the inflamed group had no spontaneous activity at 32 °C. Once stimulus temperature dropped, even by <0.5 °C, cold fibers quickly increased their discharge rate up to near 100 Hz (instantaneous frequency, see Fig. 4, left panel) irrespective of the existence of resting discharge at 32 °C. When the stimulus temperature reached the noxious range (<15 °C), the discharge rate decreased, and in some cases the discharge even disappeared completely. There was no significant difference in the cooling response between the control and inflamed groups at any time (data not shown).

Next, we analyzed the heat response of C-cold units. These fibers usually showed continuous activity at normal skin temperature as described above. When a heat ramp was started, they immediately stopped firing, although some showed 'paradoxical discharge' when heated further to >47 °C. In the current study, 6 out of 8 units from the inflamed group showed the paradoxical discharge, while 4 out of 12 units from the control group did. The proportion of paradoxical discharge-positive units seems to be higher in the inflamed group, but the difference was not statistically significant ($P = 0.085$). The 'heat thresholds' of these units did not differ, either (46.1 ± 1.0 and 47.8 ± 1.2 °C, respectively; $P > 0.05$).

4. Discussion

The major finding of the present study is that the cold response is facilitated in two types of C-primary afferent fibers (CLTMs and C-nociceptors) in persistently inflamed rats. It might be reasonable to conclude that this change is not mediated by hypoxia resulting from cold-induced constriction of blood vessels, because the controlled cold stimulation was used for control as well as for inflamed preparations.

In contrast to the changed sensitivity to cold of cutaneous CLTM and C-nociceptors, the heat response of nociceptors was not facilitated in these animals (2–3 weeks after inoculation of CFA) even though inflammation persisted. This observation is in accordance with the previous observation that showed disappearance of heat hyperalgesia in 5 days after CFA inoculation (Hylden et al., 1989). The mechanical threshold of nociceptors measured with nylon monofilaments did not differ between the two groups, either. CLTM units were excited by the weakest nylon monofilaments used in both groups; thus, smaller differences in mechanical threshold would not have been detected. However, CLTMs of inflamed animals showed higher activities when the thermode was placed on the receptive field. This observation might indicate increased sensitivity of this receptor to mechanical stimulation in inflamed tissue. In the following section, we discuss the changed cold responses of the two types of C-afferent neurons (CLTMs and nociceptors) studied.

4.1. Low-threshold mechanoreceptors

We found that innocuous cold of 25 °C evoked increased nociceptive behavior in persistently inflamed rats. The present experimental responses are considered to have simulated the symptoms in human patients exposed to moderate cold. The time course of development of this cold allodynia is similar to that of the cold hyperalgesia observed in rats given subcutaneous injection of mycobacterium tuberculosis to the hind paw, using a 5 °C cold plate (Jasmin et al., 1998).

This study is the first to show that the cold response of CLTM units was increased in inflamed rats, and interestingly, that their maximum response to cold was observed at about 27–23 °C, temperatures that are innocuous and close to that used for the behavioral pain test. We also found that the proportion of cold-responsive C-nociceptors increased in inflamed rats, but their cold threshold was 10.0 ± 2.6 °C, which is nearly noxious and far below the temperature used for the behavioral test. These findings together might suggest that facilitated response of CLTM units is involved in the increased number of paw shakes in response to 25 °C cold stimuli. Change in the response magnitude of CLTM was, though statistically significant, small; therefore, implication of another fiber type(s) cannot be excluded.

Under normal conditions, these CLTM neurons are considered to convey sensations of light touch, such as gentle,

slow stroking (Bessou and Perl, 1969). A recent finding even suggests that their activation induces a pleasant sensation (Olausson et al., 2002). However, in pathological conditions, these neurons may be involved in pain signaling, assisted by alterations in the central nervous system. Myelinated afferent fibers, which normally convey information of light touch and pressure, have well documented involvement in pain signaling after axotomy and inflammation. A proposed mechanism for this is A-fiber sprouting into the lamina II in the spinal cord (Woolf et al., 1992; Koerber et al., 1994). Besides, sprouting of C-fibers is reported to be induced by nerve growth factor (NGF) (Diamond et al., 1992), which increases in the nervous tissues in rats with hind paw inflammation induced by Freund's adjuvant (Donnerer et al., 1992; Kasai and Mizumura, 1999). CLTMs are reported to terminate in the lamina II in normal guinea pigs (Sugiura et al., 1986). They also may form new synaptic contacts or strengthen the pre-existing contacts with nociceptive secondary neurons in inflamed conditions, and transmit pain. Such morphological and/or functional changes may have occurred in inflamed animals, and excitation of CLTMs might have induced nociceptive behaviors. Elucidation of this point will require further study in the future.

The mechanism of facilitated cold sensitivity of CLTMs remains a matter of speculation: the mechanical transducer channel of CLTMs might be sensitive to cold, or it might detect mechanical change induced by temperature decrease and the activity of this channel might be modulated by some inflammatory mediators. The latter possibility is supported by the fact that a temperature decrease but not absolute cold temperature can be a stimulus to CLTMs. One of the candidates for this channel would be DRASIC, which is considered to play some role in mechanical transduction (Price et al., 2001) and has sensitivity to cold (Askwith et al., 2001). Another candidate would be TREK-1, described in the next section. Alternatively, some cold transducer channel might be expressed in CLTMs, and the activity of this channel might be modulated after inflammation.

4.2. C-nociceptors

The percentage of cold-responsive C-nociceptors significantly increased in monoarthritic rats in the present experiment. Changed sensitivity to mechanical and/or heat in inflamed conditions or after repetitive stimulation has been well documented (Schaible and Schmidt, 1988; Häbler et al., 1990; Koltzenburg et al., 1999), but there have been no reports on changed cold sensitivity in inflammation. Therefore, the present report is the first to demonstrate altered cold sensitivity of nociceptors in inflammation.

The threshold temperature of nociceptors in response to cold was $10.0 \pm 2.6\,^{\circ}C$ in the inflamed rats, far below the temperature used for the current behavioral test. There are several reports showing that persistent inflammation elicits cold hyperalgesia. Perrot et al. (1993) reported that struggle latency in response to immersion in 10 °C water decreased in polyarthritic rats. In addition, Jasmin et al. (1998) reported that the number of paw lifts on a 5 °C cold plate increased in monoarthritic rats. The presently observed change in cold sensitivity in nociceptors might be responsible for the hyperalgesia to noxious cold observed in these earlier reports.

How was the proportion of nociceptors sensitive to cold increased? There would seem to be two possibilities. One is that the cold threshold of seemingly cold-insensitive units shifted to a higher temperature. Some nociceptors might have had a threshold below 2 °C (Simone and Kajander, 1996), the lowest temperature used in the present experiment, and so appear to be cold insensitive. These units might then have been sensitized, and become sensitive to cold >2 °C. Another possibility is that originally cold-insensitive units acquired new cold sensitivity.

One possible mechanism for lowered cold threshold of C-nociceptors is modulation by inflammatory mediators, similar to the sensitization of nociceptors to heat by bradykinin (Kumazawa et al., 1991; Sugiura et al., 2002). The cold transducers already identified or as-yet unidentified might also be modified by inflammatory mediator(s). A possible candidate for the inflammatory mediator that may induce cold hypersensitivity is glutamate. Leung et al. (2000) reported that intravenous application of ketamine, an NMDA receptor antagonist, ameliorated cold allodynia in human neuropathic patients, and they briefly discussed the possibility of its action in the periphery. The existence of the NMDA receptor in cutaneous unmyelinated sensory axons, the nociceptive behavior of rats in response to subcutaneously applied glutamate (Carlton et al., 1998) and the existence of glutamate at peripheral sites of inflammation (Omote et al., 1998) suggest the possibility that glutamate is associated with cold hyperalgesia in inflammation. Whether or not these inflammatory mediators modulate cold sensitivity of C-nociceptors should be addressed in future studies.

It was recently demonstrated that blockade of 4-AP-sensitive K^+ channels (IKD) alters the cold-insensitive trigeminal ganglion neurons so that they become cold sensitive (Viana et al., 2002). This might also be a possible mechanism for the increased number of cold sensitive nociceptors. Some inflammatory mediators might block this K^+ channel.

The molecular substrates of cold transduction are now being clarified. One of them is TREK-1, an outward rectifier K^+ channel (Fink et al., 1996; Maingert et al., 2000; Koh et al., 2001) sensitive to mechanical events; another is CMR1, a non-selective cation channel (McKemy et al., 2002; Peier et al., 2002) sensitive to menthol. Besides, Story et al. (2003) reported quite recently another cold sensitive ion channel, ANKTM1, a distant family member of TRP channels. Increased or de novo expression of these molecules would explain the increased percentage of cold sensitive nociceptors in the monoarthritic rat. However, the optimum temperatures for activation of the TREK-1 and CMR1 do not completely match that for C-nociceptor channels. The TREK-1 current is strongly suppressed at 22 °C, and little suppression is observed with further decreases

in temperature (Maingert et al., 2000). The CMR1 current reaches its maximum at about 10 °C, and no further increases are seen when the temperature is decreased (McKemy et al., 2002; Peier et al., 2002). By contrast, the majority of C-nociceptors were not excited by 2 °C cold in normal animals in the current experiment, and a considerable number of C-nociceptors had cold thresholds lower than 10 °C (or even <0 °C) in other experiments in the normal rat (Simone and Kajander, 1996). On the other hand, the cold response of ANKTM1 starts at 17 °C and increases along the temperature decrease down to at least 5 °C. As this ion channel is expressed in a subpopulation of nociceptive neurons (Story et al., 2003), it might be implicated in the cold hypersensitivity in nociceptive neurons observed in this study. Further studies are needed to determine the molecular mechanism of cold transduction.

In conclusion, the facilitated cold response of CLTM units might be associated to the cold allodynia to innocuous cooling seen in the current behavioral experiment, while that of C-nociceptive units might be involved with hyperalgesia to noxious cold. The cold transduction mechanism might be altered at the primary afferent level. To prove this hypothesis, further research (e.g. expression of transducer molecules and/or their functional modulation, etc.) should be done.

Acknowledgements

This work was partly supported by a Grant-in-Aid for Scientific Research (B) (KAKENHI No. 11470016) from the Japan Society for the Promotion of Science, and a Health and Labour Sciences Research Grant from Ministry of Health, Labour and Welfare. The authors are grateful to Dr. Tomoko Koeda and Mr. Toru Taguchi for their kind help in the experiments.

References

Andrew, D., Greenspan, J.D., 1999. Mechanical and heat sensitization of cutaneous nociceptors after peripheral inflammation in the rat. J. Neurophysiol. 82, 2649–2656.

Askwith, C.C., Benson, C.J., Welsh, M.J., Snyder, P.M., 2001. DEG/ENaC ion channels involved in sensory transduction are modulated by cold temperature. Proc. Natl. Acad. Sci. 98, 6459–6463.

Attal, N., Jazat, F., Kayser, V., Guilbaud, G., 1990. Further evidence for 'pain-related behaviours' in a model of unilateral peripheral mononeuropathy. Pain 41, 235–251.

Attal, N., Filliatreau, G., Perrot, S., Jazat, F., Di Giamberardino, L., Guilbaud, G., 1994. Behavioural pain-related disorders and contribution of the saphenous nerve in crush and chronic constriction injury of the rat sciatic nerve. Pain 59, 301–312.

Bessou, P., Perl, E.R., 1969. Response of cutaneous sensory units with unmyelinated fibres. J. Neurophysiol. 32, 1025–1043.

Bessou, P., Burgess, P.R., Perl, E.R., Taylor, C.B., 1971. Dynamic properties of mechanoreceptors with unmyelinated (C) fibers. J. Neurophysiol. 34, 116–131.

Butler, S.H., Godefroy, F., Besson, J.-M., Weil-Fugazza, J., 1992. A limited arthritic model for chronic pain studies in the rat. Pain 48, 73–81.

Cain, D.M., Wacnik, P.W., Turner, M., Wendelschafer-Crabb, G., Kennedy, W.R., Wilcox, G.L., Simone, D.A., 2001. Functional interactions between tumor and peripheral nerve: changes in excitability and morphology of primary afferent fibers in a murine model of cancer pain. J. Neurosci. 21, 9367–9376.

Carlton, S.M., Zhou, S., Coggeshall, R.E., 1998. Evidence for the interaction of glutamate and NK1 receptors in the periphery. Brain Res. 790, 160–169.

Diamond, J., Holmes, M., Coughlin, M., 1992. Endogenous NGF and nerve impulses regulate the collateral sprouting of sensory axons in the skin of the adult rat. J. Neurosci. 12, 1454–1466.

Donnerer, J., Schuligoi, R., Stein, C., 1992. Increased content and transport of substance P and calcitonin gene-related peptide in sensory nerves innervating inflamed tissue: evidence for a regulatory function of nerve growth factor in vivo. J. Neurosci. 49, 693–698.

Drane, D., Berry, G., Bieri, D., McFarlane, A.C., Brooks, P., 1997. The association between external weather conditions and pain and stiffness in women with rheumatoid arthritis. J. Rheumatol. 24, 1309–1316.

Fink, M., Duprat, F., Lesage, F., Reyes, R., Romey, G., Heurteaux, C., Lazdunski, M., 1996. Cloning, functional expression and brain localization of a novel unconventional outward rectifier K^+ channel. EMBO J. 15, 6854–6862.

Forster, C., Handwerker, H.O., 1990. Automatic classification and analysis of microneurographic spike data using a PC/AT. J. Neurosci. Methods 31, 109–118.

Häbler, H.-J., Jänig, W., Koltzenburg, M., 1990. Activation of unmyelinated afferent fibres by mechanical stimuli and inflammation of the urinary bladder in the cat. J. Physiol. 425, 545–562.

Handwerker, H.O., Kilo, S., Reeh, P.W., 1991. Unresponsive afferent nerve fibres in the sural nerve of the rat. J. Physiol. 435, 229–242.

Hensel, H., Iggo, A., Witt, I., 1960. A quantitative study of sensitive cutaneous thermoreceptors with C afferent fibres. J. Physiol. 153, 113–126.

Hylden, J.L.K., Nahin, R.L., Traub, R.J., Dubner, R., 1989. Expansion of receptive fields of spinal lamina I projection neurons in rats with unilateral adjuvant-induced inflammation: the contribution of dorsal horn mechanism. Pain 37, 229–243.

Iggo, A., 1969. Cutaneous thermoreceptors in primates and sub-primates. J. Physiol. 200, 403–430.

Jahanshahi, M., Pitt, P., Williams, I., 1989. Pain avoidance in rheumatoid arthritis. J. Psychosom. Res. 33, 579–589.

Jamison, R.N., Anderson, K.O., Slater, M.A., 1995. Weather changes and pain: perceived influence of local climate on pain complaint in chronic patients. Pain 61, 309–315.

Jasmin, L., Kohan, L., Franssen, M., Janni, G., Goff, J.R., 1998. The cold plate as a test of nociceptive behaviors: description and application to the study of chronic neuropathic and inflammatory pain models. Pain 75, 367–382.

Kasai, M., Mizumura, K., 1999. Endogenous nerve growth factor increases the sensitivity to bradykinin in small dorsal root ganglion neurons of adjuvant inflamed rats. Neurosci. Lett. 272, 41–44.

Kocher, L., Anton, F., Reeh, P.W., Handwerker, H.O., 1987. The effect of carrageenan-induced inflammation on the sensitivity of unmyelinated skin nociceptors in the rat. Pain 29, 363–373.

Koerber, H.R., Mirnics, K., Brown, P.B., Mendell, L.M., 1994. Central sprouting and functional plasticity of regenerated primary afferents. J. Neurosci. 14, 3655–3671.

Koh, S.D., Monaghan, K., Sergeant, G.P., Ro, S., Walker, R.L., Sanders, K.M., Horowitz, B., 2001. TREK-1 regulation by nitric oxide and cGMP-dependent protein kinase. J. Biol. Chem. 276, 44338–44346.

Koltzenburg, M., Bennett, D.L.H., McMahon, S.B., 1999. Neutralization of endogenous NGF prevents the sensitization of nociceptors supplying inflamed skin. Eur. J. Neurosci. 11, 1698–1704.

Kumazawa, T., Mizumura, K., Minagawa, M., Tsujii, Y., 1991. Sensitizing effects of bradykinin on the heat responses of visceral nociceptor. J. Neurophysiol. 66, 1819–1824.

Leem, J.W., Willis, W.D., Chung, J.M., 1993. Cutaneous sensory receptors in the rat foot. J. Neurophysiol. 69, 1684–1699.

Leung, A., Wallace, M.S., Ridgeway, B., Yaksh, T., 2000. Concentration–effect relationship of intravenous alfentanil and ketamine on peripheral neurosensory thresholds, allodynia and hyperalgesia of neuropathic pain. Pain 91, 177–187.

Lewis, A.J., Carlson, R.P., Chang, J., 1985. Experimental model of inflammation. In: Bonta, I.L., Bray, M.A., Parnham, M.J. (Eds.), The Pharmacology of Inflammation. Handbook of Inflammation, vol. 5. Elsevier, New York, pp. 371–397.

Maingert, F., Lauritzen, I., Patel, A.J., Heurteaux, C., Reyes, R., Lesage, F., Lazdunski, M., Honoré, E., 2000. TREK-1 is a heat-activated background K^+ channel. EMBO J. 19, 2483–2491.

McKemy, D.D., Neuhausser, W.M., Julius, D., 2002. Identification of a cold receptor reveals a general role for TRP channels in thermosensation. Nature 416, 52–58.

Mizumura, K., 1998. Natural history of nociceptor sensitization—the search for a peripheral mechanism of hyperalgesia. Pain Rev. 5, 59–82.

Mizumura, K., Kumazawa, T., 1996. Modification of nociceptor responses by inflammatory mediators and second messengers implicated in their action—a study in canine testicular polymodal receptors. In: Kumazawa, T., Kruger, L., Mizumura, K. (Eds.), The Polymodal Receptor—A Gateway to Pathological Pain. Elsevier, Amsterdam, pp. 115–141.

Neto, F.L., Schadrack, J., Platzer, S., Zieglgänsberger, W., Tölle, T.R., Castro-Lopes, J.M., 2000. Expression of metabotropic glutamate receptors mRNA in the thalamus and brainstem of monoarthritic rats. Mol. Brain Res. 81, 140–154.

Olausson, H., Lamarre, Y., Backlund, H., Morin, C., Wallin, B.G., Starck, G., Ekholm, S., Strigo, I., Worsley, K., Vallbo, Å.B., Bushnell, M.C., 2002. Unmyelinated tactile afferents signal touch and project to insular cortex. Nat. Neurosci. 5, 900–904.

Omote, K., Kawamata, T., Kawamata, M., Namiki, A., 1998. Formalin-induced release of excitatory amino acids in the skin of the rat hind paw. Brain Res. 787, 161–164.

Peier, A.M., Moqrich, A., Hergarden, A.C., Reeve, A.J., Anderson, D.A., Story, G.M., Earley, T.J., Dragoni, I., McIntyre, P., Bevan, S., Patapoutian, A., 2002. A TRP channel that senses cold stimuli and menthol. Cell 108, 705–715.

Perrot, S., Attal, N., Ardid, D., Guilbaud, G., 1993. Are mechanical and cold allodynia in mononeuropathic and arthritic rats relieved by systemic treatment with calcitonin or guanethidine? Pain 52, 41–47.

Price, M.P., McIlwrath, S.L., Xie, J., Cheng, C., Qiao, J., Tarr, D.E., Sluka, K.A., Brennan, T.J., Lewin, G.R., Welsh, M.J., 2001. The DRASIC cation channel contributes to the detection of cutaneous touch and acid stimuli in mice. Neuron 32, 1071–1083.

Ritchie, J.M., Douglas, W.W., 1957. A technique for recording functional activity in specific groups of medullated and non-medullated fibres in whole nerve trunks. J. Physiol. 138, 19–30.

Sato, J., Morimae, H., Takanari, K., Seino, Y., Okada, T., Suzuki, M., Mizumura, K., 2000. Effects of lowering ambient temperature on pain-related behaviors in a rat model of neuropathic pain. Exp. Brain Res. 133, 442–449.

Schaible, H., Schmidt, R.F., 1988. Time course of mechanosensitivity changes in articular afferents during a developing experimental arthritis. J. Neurophysiol. 60, 2180–2195.

Shea, V.K., Perl, E.R., 1985. Sensory receptors with unmyelinated C-fibers innervating the skin of the rabbit's ear. J. Neurophysiol. 54, 491–501.

Simone, D.A., Kajander, K.C., 1996. Excitation of rat cutaneous nociceptors by noxious cold. Neurosci. Lett. 213, 53–56.

Simone, D.A., Kajander, K.C., 1997. Responses of cutaneous A-fiber nociceptors to noxious cold. J. Neurophysiol. 77, 2049–2060.

Spray, D.C., 1986. Cutaneous temperature receptors. Ann. Rev. Physiol. 48, 625–638.

Story, G.M., Peier, A.M., Reeve, A.J., Eid, S.R., Mosbacher, J., Hricik, T.R., Earley, T.J., Hergarden, A.C., Andersson, D.A., Hwang, S.W., McIntyre, P., 2003. ANKTM1, a TRP-like channel expressed in nociceptive neurons, is activated by cold temperatures. Cell 112, 819–829.

Sugiura, Y., Lee, C.L., Peier, A.M., 1986. Central projections of identified, unmyelinated (C) afferent fibers innervating mammalian skin. Science 234, 358–361.

Sugiura, T., Tominaga, M., Katsuya, H., Mizumura, K., 2002. Bradykinin lowers the threshold temperature for heat activation of vanilloid receptor 1. J. Neurophysiol. 88, 544–548.

Takahashi, K., Sato, J., Mizumura, K., 2002. Responses of primary afferent C-fibers to cold were facilitated in the adjuvant-monoarthritic rats hyperalgesic to cold. Jpn. J. Physiol. 52, S153–S153.

Viana, F., de la Pena, E., Belmonte, C., 2002. Specificity of cold thermotransduction is determined by differential ionic channel expression. Nat. Neurosci. 5, 254–260.

Vrinten, D.H., Gispen, W.H., Groen, G.J., Adan, R.A.H., 2000. Antagonism of the melanocortin system reduces cold and mechanical allodynia in mononeuropathic rats. J. Neurosci. 20, 8131–8137.

Woolf, C.J., Shortland, P., Coggeshall, R.E., 1992. Peripheral nerve injury triggers central sprouting of myelinated afferents. Nature 355, 75–78.

Yashpal, K., Fisher, K., Chabot, J.-G., Coderre, T.J., 2001. Differential effects of NMDA and group I mGluR antagonists on both nociception and spinal cord protein kinase C translocation in the formalin test and a model of neuropathic pain in rats. Pain 94, 17–29.

Available online at www.sciencedirect.com

SCIENCE DIRECT®

SAUNDERS

European Journal of Pain 7 (2003) 493–505

www.EuropeanJournalPain.com

Nerve terminals extend into the temporomandibular joint of adjuvant arthritic rats

Masamichi Shinoda [a,b], Takashi Honda [c], Noriyuki Ozaki [b], Hisashi Hattori [a], Hideki Mizutani [a], Minoru Ueda [a], Yasuo Sugiura [b,*]

[a] *Department of Oral and Maxillofacial Surgery, Nagoya University Graduate School of Medicine, Nagoya, Japan*
[b] *Department of Functional Anatomy and Neuroscience, Nagoya University Graduate School of Medicine, Nagoya, Japan*
[c] *Department of Anatomy and Histology, Fukushima Medical University School of Medicine, Fukushima, Japan*

Received 14 August 2002; accepted 25 February 2003

Abstract

The innervation of the temporomandibular joint (TMJ) has attracted particular interest because of the close association with complex mandibular movement. Although the pathological changes of disk innervation may have a crucial role in the development of TMJ pain, the innervation of the TMJ disk by experimentally induced arthritis has rarely been examined in detail. Arthritic rats were induced by injection with 0.1 ml solution of Complete Freund's adjuvant (CFA). We investigated three-dimensional distribution of nerve fibers in the TMJ disk using immunohistochemistry for protein gene product-9.5 (PGP-9.5) and calcitonin gene-related peptide (CGRP) in naive and arthritic rats. To clarify the possible role of nerve growth factor (NGF) and its receptor on changes in peripheral innervation of the TMJ, the expressions of trkA and p75 receptor in trigeminal ganglia were examined. Although PGP-9.5 and CGRP immunoreactive (ir) fibers were seen in the peripheral part of the TMJ disk, they were not seen in its central part. The total length and the length density of PGP-9.5 ir and CGRP ir nerve fibers increased in arthritic rats. The innervation area of fibers proliferating in the rostro-medial part merged with that of fibers in the rostro-lateral part in the arthritic rats. In addition, the ratio of trkA- and p75-positive small- and medium-sized cells increased in trigeminal ganglia. It is assumed that increasing innervation of the TMJ disk may be important for the pathophysiology of TMJ pain. NGF and its receptors are likely involved in pathological changes of the TMJ disk.

Keywords: TMJ disk; PGP-9.5; CGRP; Trigeminal ganglion; Complete Freund's adjuvant arthritis

1. Introduction

The temporomandibular joint (TMJ) consists of the temporal articular tubercle, the mandibular fossa in the upper part, and the mandibular condyle in the lower part. The TMJ disk is an oval plate of fibrous tissue, which completely divides the TMJ into its upper and lower parts. Many muscles in this joint produce complicated joint movements including depression, elevation, protrusion, retraction and lateral movement. These peculiar arthrological features of the TMJ indicate that the TMJ disk accepts various kinds of pathological stress in mobility. It is important to understand the physiological and pathological aspects of the TMJ, especially the innervation of the TMJ disk in patients suffering from temporomandibular joint disorders (TMD).

Previous studies reported various results regarding the innervation of the TMJ disk and the synovial membrane of the TMJ. Nerve fibers reportedly extended into the synovial villus and contacted the synovial cells of the TMJ disk in monkeys (Keller and Moffett, 1968). No nerve fiber was found in the synovial lining layer of the mouse TMJ disk (Dreessen et al., 1990), even at the electron-microscopic level. Virtually all morphological observations of the innervation of the TMJ disk have

* Corresponding author. Tel.: +81-52-744-2014; fax: +81-52-744-2027.
E-mail address: ysugiura@med.nagoya-u.ac.jp (Y. Sugiura).

1090-3801/$30
doi:10.1016/S1090-3801(03)00021-1

been obtained from silver impregnation techniques. However, silver impregnation does not stain nerve fibers specifically (Fundin et al., 1995). Current immunohistochemical studies have served to identify the peptidergic innervation in the TMJ disk and its surrounding soft tissues. Substance P (SP)-like immunoreactive (ir) fibers exist in the joint capsule, disk attachment, and periosteum in monkey TMJ (Johansson et al., 1986). The central part of the TMJ disk contains no nerve fibers from postnatal days 0 through 24 (Shimizu et al., 1996). Although these studies have described the distribution of nerve fibers, the pathological changes of innervation over the whole body of the TMJ disk are still unclear.

Recent arthroscopic and histopathological investigations on painful TMJ in humans have demonstrated the occurrence of inflammatory reactions in synovial membrane (Murakami et al., 1991). Experimental models of arthritis have been available for clarifying the initial stage of the inflammatory process. Several studies have documented morphological changes in the synovial membrane (Nozawa-Inoue et al., 1998) or other periarticular tissues (Kapila et al., 1995; Kapila and Xie, 1998) of the TMJ following experimentally induced arthritis in animals. Other investigations have shown increasing concentrations of tachykinins or prostaglandins in the synovial fluid of the inflamed TMJ (Alstergren and Kopp, 1997; Appelgren et al., 1998; Carleson et al., 1997; Swift et al., 1998). Although these studies have described pathological changes in the TMJ and surrounding tissue, changes in innervation of the TMJ disk in experimental arthritis have not been extensively studied.

Nerve growth factor (NGF) is the prototypic molecule of the neurotrophin family of polypeptide trophic factors. NGF has been established as a required trophic factor for the differentiation and survival of sympathetic and some sensory neurons in the peripheral system (Barde, 1989). In addition to its effect on neuronal survival, NGF locally regulates the amount of axonal branching (Campenot, 1987). For example, injury to tooth pulp often results in extensive sprouting of sensory nerve fibers at the site of wound repair in response to the local increase in NGF concentration (Byers et al., 1990; Byers et al., 1992). Increased expression of NGF has also been implicated in the nociceptive response (Dyck et al., 1997; Wheeler et al., 1998). When NGF was induced in the peripheral tissue, the NGF receptor (trkA and p75 receptor) on the membranes of responsive neurons would change in the peripheral nervous system. A recent study has indicated that trkA expression increased in the trigeminal ganglia innervated in injured teeth by retrograde transport of NGF (Wheeler and Bothwell, 1992).

In the present study, we investigated nerve distribution to clarify the changes under pathological conditions, and the overall features of innervation were examined in the TMJ disk of both naive and complete Freund's adjuvant (CFA) arthritic rats. In addition, to clarify the possible role of NGF and its receptor on changes of peripheral innervation in the TMJ, the expressions of trkA and p75 receptor in trigeminal ganglia were examined in the CFA arthritic rats. Characterization of this molecular system that mediates both repair and pain perception is important to develop novel clinical tools for promoting repair and relief of TMJ pain.

2. Methods

2.1. Animals

Twenty-five male Lewis rats weighing around 230 g were used in this study. Rats were exposed to a light–dark cycle (L:D 12:12-h) and kept in a temperature-controlled room (23 °C). This study was conducted in accordance with the guidelines of the International Association for the Study of Pain (Zimmermann, 1983).

2.2. Complete Freund's adjuvant arthritis

Under anesthesia with inhalation of diethyl ether, twenty rats were intracutaneously injected with 0.1 ml solution of CFA at both the parietal scalp and base of tail (Nozawa-Inoue et al., 1998). The adjuvant solution contained 6 mg of heat-killed *Mycobacterium butyricum* (Difco Laboratories, Detroit, MI, USA) in 1 ml of paraffin oil (Wako, Tokyo, Japan). After the injection, rats were given laboratory chow and tap water ad libitum in conventional laboratory conditions. Five non-treated naive rats weighing around 230 g were used as the control. Sequential changes in body weight, food and water consumption were measured daily in five CFA-treated rats and five naive rats. Five rats each were sacrificed at 2, 3, 4 and 5 weeks post-CFA injection for immunohistochemistry of trigeminal ganglia. The immunohistochemistry was carried out for the TMJ disks of five rats sacrificed at 5 weeks post-CFA injection.

2.3. Tissue preparation

Rats were anesthetized with an intraperitoneal injection of sodium pentobarbital (50 mg/kg, Nembutal, Abbot Laboratories, Chicago, IL, USA), and transcardially perfused with heparinized saline followed by a cold fixative containing 4% paraformaldehyde in 0.1 M phosphate buffer (PB, pH 7.4). Bilateral TMJ and trigeminal ganglia were immediately dissected out after perfusion, and immersed in the same fixative for 4 h at 4 °C. The TMJ disk with its surrounding synovial tissues was carefully removed from the maxillary and mandibular bones. Post-fixed disks were rinsed with 0.1 M

phosphate-buffered saline (PBS) and dehydrated through an ascending series of ethanol (70%, 80%, 90%, 95%, 100%). Disks were then delipidized with xylene until they became transparent, and were rehydrated with a descending series of ethanol to PBS (pH 7.4).

To visualize the pathological changes after CFA treatment, tissues of TMJ in the naive and 5-week rats after CFA treatment were stained by Hematoxylin–Eosin.

Post-fixed trigeminal ganglia were kept in PBS containing 20% sucrose for cryoprotection. The specimens were then embedded in Tissue Mount (Chiba Medical, Japan) and stored until cryosectioning at −30 °C.

The trigeminal ganglia were cut in the horizontal plane along the long axis of the ganglion on a cryostat at a thickness of 15 μm. Every twentieth section – approximately five sections per trigeminal ganglion – was chosen for each rat. In the trigeminal ganglia at 5-weeks post-CFA injection, the frozen trigeminal ganglia were serially cut. Sections were mounted on glass slides coated with chrome alum gelatin and dried at room temperature overnight.

2.4. Immunohistochemistry

2.4.1. TMJ disk

Anti-PGP-9.5 rabbit IgG against synthetic rat PGP-9.5 (Ultra Clone, UK) and anti-CGRP rabbit IgG against synthetic rat CGRP (Serotec, Japan) were used as a primary antibody. Each antibody was diluted at a concentration of 1:1000 in 0.1 M PBS containing 4% normal goat serum and 0.3% Triton X-100 (Sigma, St. Louis, MO, USA). Whole tissues of the TMJ disk were incubated in a solution of either anti-PGP-9.5 or anti-CGRP antisera for a week at 4 °C.

After rinsing with 0.1 M PBS, all samples were reacted with biotinylated goat anti-rabbit IgG (Vector Laboratories, Burlingame, CA, USA) at a dilution of 1:200 in 0.1 M PBS for 2 h at 4 °C. After rinsing with 0.1 M PBS, they were immersed in a solution of avidin and biotin–peroxidase complex (Vector Laboratories) at a dilution of 1:100 in 0.1 M PBS for 90 min at 4 °C. Disks were then immersed in PBS containing 0.1% 3,3′-diaminobenzidine dihydrochloride (DAB) (Sigma). Antigen-binding sites were made visible by adding 0.004% hydrogen peroxide. After staining, disks were treated with 0.05% osmium for 30 min at room temperature. As a control, the TMJ disk of another CFA arthritis rat was processed using rabbit serum without each primary antiserum using the same process described above.

Immunoreactive fibers in the TMJ disk were manually traced, and reconstructed three-dimensionally by a light microscope-equipped, computer-aided imaging system (Neurolucida, MicroBrigthtfield, VT, USA). This system allows three-dimensional mapping of nerve fibers within thick TMJ disk while focusing and tracing fibers by using stage position encoders. The total length of ir fibers were automatically calculated by this system. The length density of nerve fibers was calculated by the formula: (total length of nerve fibers (mm)/area of TMJ disk (mm^2)).

2.4.2. Trigeminal ganglia

For the immunohistochemistry of trigeminal ganglia, anti-trkA rabbit IgG against synthetic rat trkA (Chemicon International, Temecula, CA, USA), anti-p75 rabbit IgG against synthetic human p75 (Promega, Madison, WI, USA) were used after dilution at a concentration of 1:1000 in 0.1 M PBS containing 4% normal goat serum and 0.3% Triton X-100 (Sigma). Sections were reacted with either anti-trkA or anti-p75 antibodies for 3 days at 4 °C. After rinsing with 0.1 M PBS, all samples were reacted with biotinylated goat anti-rabbit IgG (Vector Laboratories) at a dilution of 1:200 in 0.1 M PBS for 2 h at 4 °C. After rinsing with 0.1 M PBS, they were immersed in a solution of avidin and biotin–peroxidase complex (Vector Laboratories) at a dilution of 1:100 in 0.1 M PBS for 90 min at 4 °C. Then, the sections were immersed in PBS containing 0.1% 3, 3′-diaminobenzidine dihydrochloride (DAB) (Sigma). Antigen-binding sites were made visible by adding 0.004% hydrogen peroxide. Diameters of the labeled cells were measured by a computer-aided imaging system (Neurolucida).

In the trigeminal ganglia at 5-weeks post-CFA injection, adjacent sections were stained with antibodies to trkA, CGRP or p75. Pairs of adjacent sections were assessed to determine double labeling of ganglion cells. The anti-trkA (Chemicon International), anti-p75 (Promega Corp) and anti-CGRP rabbit IgG (Serotec) were used for primary antibody after dilution at a concentration of 1:1000 in 0.1 M PBS containing 4% normal goat serum and 0.3% Triton X-100 (Sigma). Antigen-binding sites were made visible by the above method.

2.5. Statistical analysis

The results were expressed as means ± standard error (SEM). Results were analyzed by Student's unpaired t test, one-way ANOVA, or two-way ANOVA for repeated measures where appropriate, followed by Tukey's test for multiple comparisons, if warranted. A P value of < 0.05 was considered significant.

3. Results

3.1. Body weight, food and water consumption

Polyarthritis was induced by CFA injection. About one week later, the elbow joints and ankles swelled, and became immobile. The rats in which CFA arthritis

showed no more body weight gain at about 250 g after CFA administration. In contrast to the arthritis group, naive rats showed a continuous increase in body weight during the experimental period (Fig. 1A). Food intake of the arthritis group was significantly decreased after CFA treatment compared to the naive rats (Fig. 1B). Also, water intake of the arthritis group was significantly lower than the naive rats at 6, 12 and 18 days (Fig. 1C).

3.2. Observations of synovial membrane

Fig. 2 showed the synovial membrane of post-inflammatory features in arthritic rats.

In arthritic rats, a few lymphatic (arrowheads) or granular cells (arrows) were scattered throughout the subintimal synovial tissue. There was no infiltration by inflammatory cells, and no proliferation of the synovium. Increased fibroblasts (white arrowheads) and dense collagenous fibers (white arrows) were observed in the synovial membrane in the arthritic rats.

3.3. Macroscopic observations of TMJ disk innervations

Three kinds of nerve bundles were found to enter the TMJ disk. The deep temporal nerve entered the joint capsule at the rostro-lateral margin of the disk. The masseteric nerve entered at the rostro-medial margin of the disk, while a nerve bundle of the auriculotemporal nerve and its small branches entered the joint capsule at the caudal margin (Fig. 3). In specimens with whole-mount preparation, immunopositive nerve fibers were observed in the similar relation to the distribution of three nerves. The distributional overlapping and nerve origins in TMJ disk are identified by tracing nerve fibers in the carefully oriented disk.

3.4. Immunohistochemical observation

Although PGP-9.5 immunoreactive (ir) fibers were found in the rostro-lateral, rostro-medial, and caudal parts of the TMJ disk in naive rats, they were not seen in the central part of the disk (Figs. 4A, B and 5A). The PGP-9.5 ir fibers took a meandering route in the rostral and caudal part of the disk, but in the medial and lateral part they showed different features; several nerve fibers forming nerve fascicles ran together and then branched off thin nerve fibers to the peripheral portion of the disk. In the medial and lateral part, on the other hand, the nerve fascicles were thin, consisted of a few fibers and branched out into a thin fiber plexus. Observations of the specimens processed immunohistochemically by whole-mount preparation methods revealed that fibers had no special terminals and showed free nerve endings.

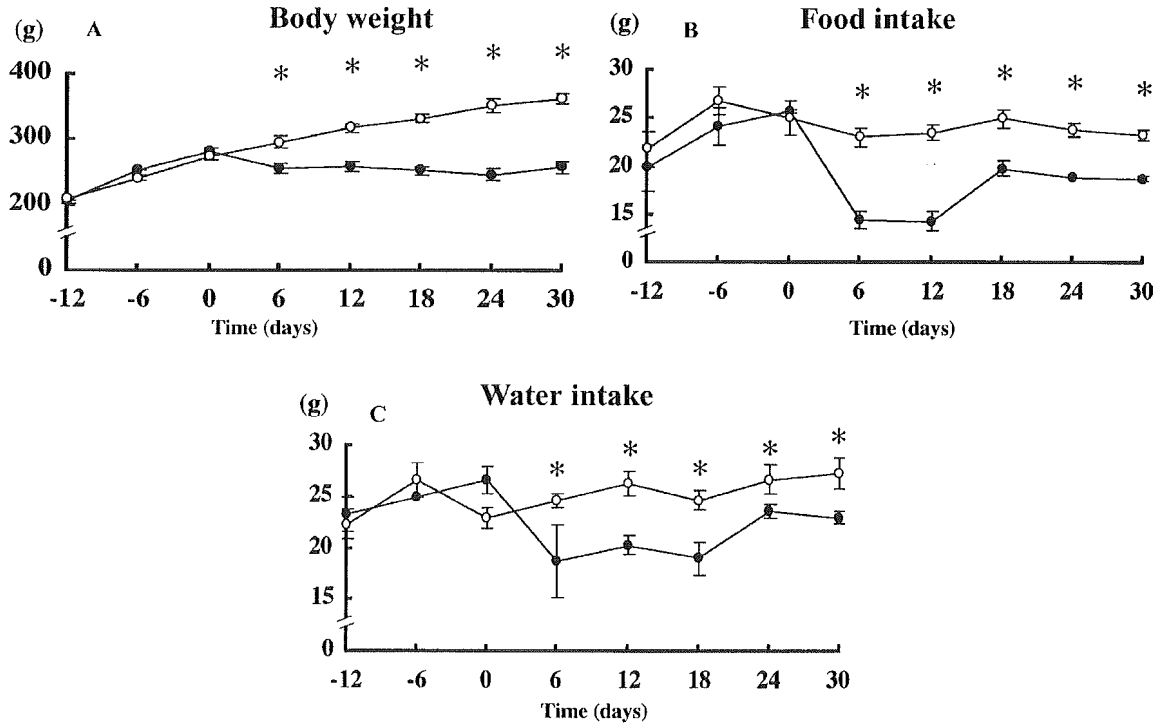

Fig. 1. Rat behavior following injections of complete Freund's adjuvant (CFA). Graphs showing changes in body weight (A), food intake (B), water intake (C). $n = 5$ for each group. Black point, CFA arthritic rats; White point, Naive rats. For statistical analysis, Student's t test and standard error were used. * $P < 0.05$.

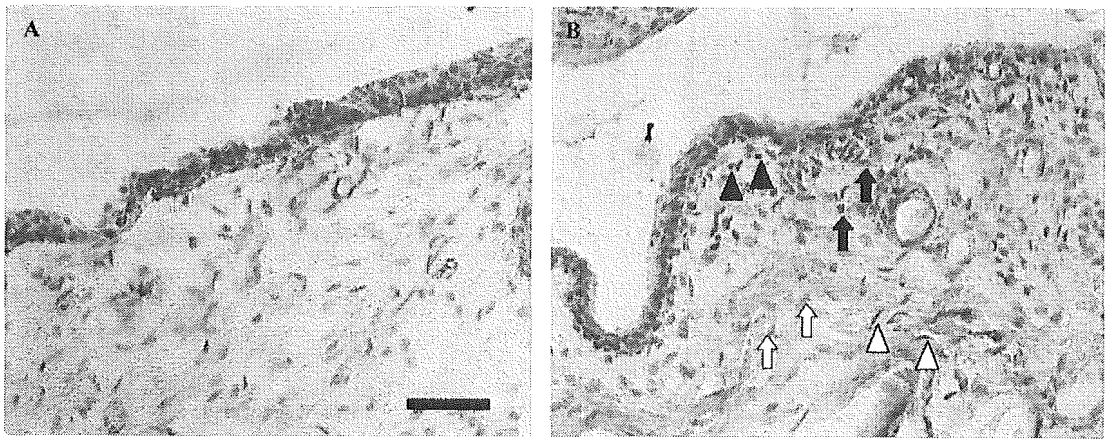

Fig. 2. Synovial membrane stained by Hematoxylin–Eosin. Naive (A), five weeks after CFA treatment (B). Lymphatic cells (arrowheads), granular cells (arrows), fibroblasts (white arrowheads) and dense collagenous fibers (white arrows) were seen in B.

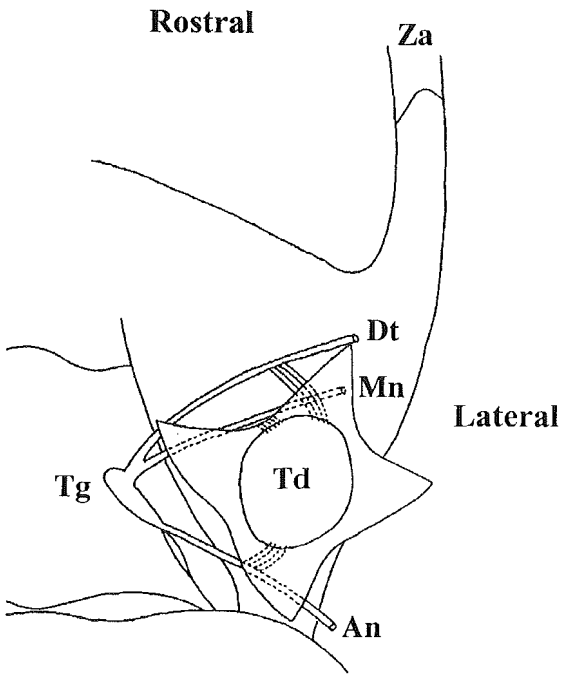

Fig. 3. Ventral aspect of the TMJ disk and peripheral tissue of left temporomandibular joint of the rat (joint capsule is open). Za, zygomatic arch; Dt, deep temporal nerve; Mn, masseteric nerve; An, auriculotemporal nerve; Td, TMJ disk; Tg, trigeminal ganglion.

In both naive and arthritic rats, nerve fibers were observed in the rostro-medial, rostro-lateral and caudal parts of the disk. In the naive rats there was no overlapping of the distribution area, whereas in the arthritic rats the proliferating fibers overlapped their distribution area (arrowheads in Fig. 5). The arthritic rats showed fiber extension toward the central part of the TMJ disk in comparison with the naive rats, in which the nerve fibers never extended to the central part of the disk (arrows in Fig. 5). The total length of PGP-9.5 ir nerve fibers increased from 80.9 to 98.1 mm in arthritic rats. Similarly, the length density increased from 9.8 to 11.8 mm/mm^2 (Fig. 6A).

Similar to PGP-9.5 ir fibers, the CGRP ir fibers were seen in the peripheral part of the TMJ disk (Figs. 4C, D and 7A). No fibers were observed in the central part of the TMJ disk. Nerve fibers meandered along the rim in the rostral and caudal parts of the TMJ disk. The distribution pattern of CGRP ir fibers was also similar to that of PGP-9.5 ir fibers. The nerve fascicles consisted of two or three nerve fibers and branched off into terminal fibers (Fig. 4C, D). Microscopic observation revealed CGRP ir nerve fibers to be thinner than PGP-9.5 ir fibers.

The length density of the CGRP ir fibers was smaller than that of the PGP-9.5 ir fibers (Fig. 6). Compared to those of the naive rats, the total length of CGRP ir fibers increased from 35.7 to 44.7 mm, and the length density increased from 4.3 to 5.4 mm/mm^2, as seen among the PGP-9.5 ir fibers in arthritic rats (Fig. 6B). The fiber distribution area in the rostro-medial part merged with that of the rostro-lateral part of the disk (Fig. 7).

3.5. Trigeminal ganglion

After the immunohistochemistry for trkA and p75 NGF receptors, immunopositive cells were stained dark or light brown in color and could be easily distinguished from the non-positive cells (arrowheads in Fig. 8). We arbitrarily classified the cell sizes according to the frequency distribution of the ganglion cells and data in the literature (Lee et al., 1985). The imaging system can measure cell size by tracing cells. TrkA- and p75-positive cells were found in varying percentages in the small to large cells in the trigeminal ganglia (Fig. 9).

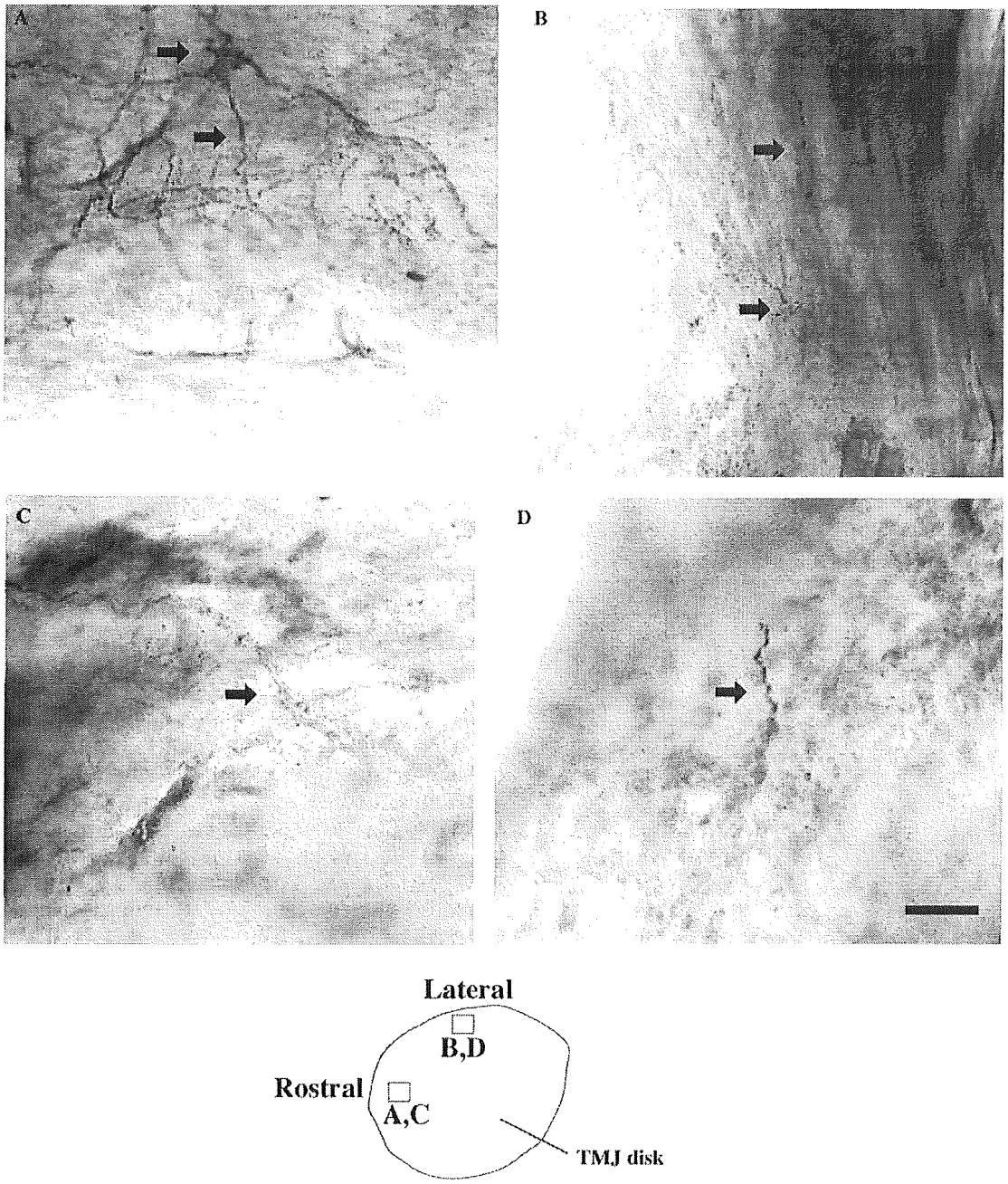

Fig. 4. Photomicrographs of PGP-9.5 (A,B) and CGRP(C,D) immunoreactive nerve fibers of the TMJ disk in the whole-mount preparation of naive rats. (A,C) rostral part, (B,D) lateral part. Arrow indicates PGP-9.5 positive (A,B) and CGRP positive (C,D) thin nerve fibers. The bottom illustration indicates the parts of the disk displayed in A, B, C and D. Size scale bar, 1 mm.

After 2 weeks of CFA treatment, the trkA-positive cells strikingly increased to 9.2% in the small cell group (< 20 μm); they showed a consistently higher level than naive rats throughout the experimental period (Fig. 9). In the medium cell group (20–30 μm), trkA-positive cells significantly increased from 3 (8.8%) through 5 (9.9%) weeks after CFA injection. In the large cell group (> 30 μm), the ratio of trkA-positive cells slightly but significantly increased at week 4 (2.3%).

Similar to the findings of trkA-positive cells, p75-positive cells in the small cell group increased to 8.9% at week 2 after CFA injection, and kept increasing after week 5. The p75-positive cells increased at week 4 (8.4%) after CFA injection in the medium cell group. There was no change in ratio of p75-positive cells in the large cell group after CFA injection (Fig. 9).

In trigeminal ganglia at week 5 after CFA injection, there were CGRP-positive cells with trkA or p75 (Fig. 10).

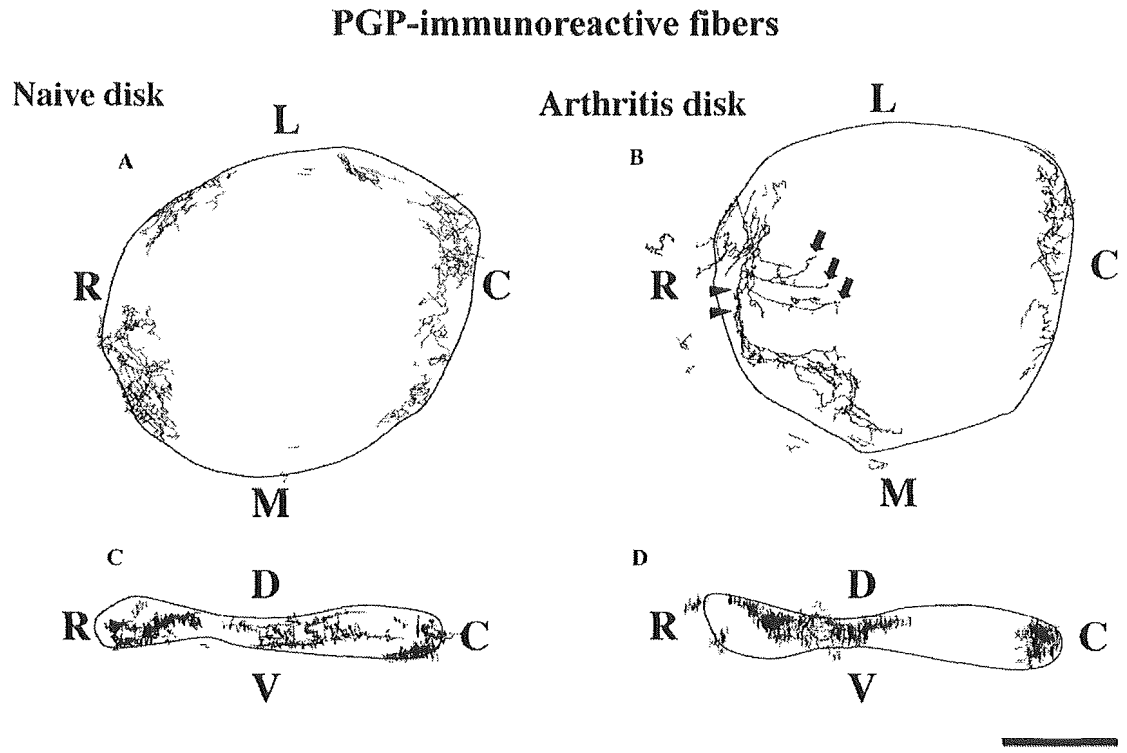

Fig. 5. Computer-aided, camera lucida drawing of PGP-9.5 immunoreactive fibers in the whole-mount preparation of the TMJ disk of naive rat (A,B) and arthritic rat (C,D). (A,C) Dorsal view. (B,D) Lateral view. R, rostral; C, caudal; D, dorsal; M, medial; V, ventral. Size scale bar, 1 mm.

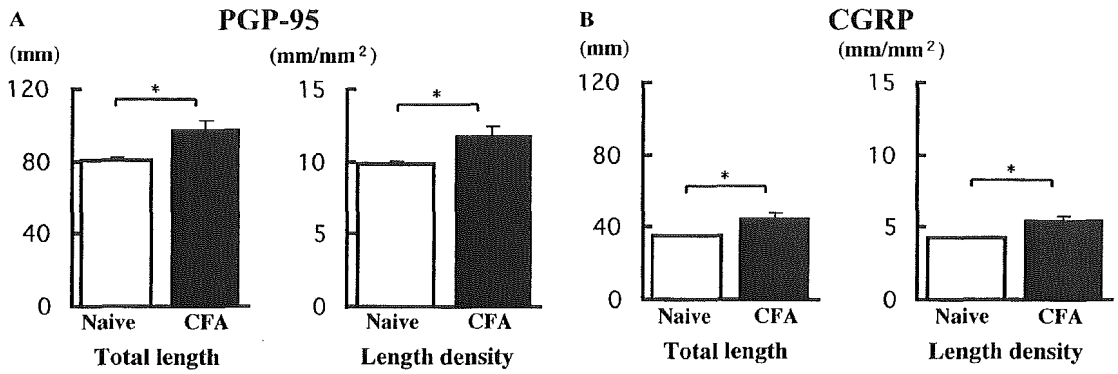

Fig. 6. Quantification of PGP-9.5 and CGRP immunoreactive fibers in the TMJ disk. Fiber length and length density were compared between the naive and CFA arthritic rats. ($n = 5$) *$P < 0.05$.

4. Discussion

4.1. Assessment of CFA arthritic rats

Body weight and food intake decreased and water intake slightly decreased in the CFA-injected groups compared with the naive rats. Food intake was especially difficult for rats probably due to the pain of TMJ arthritis, whereas their water intake was less affected because only slight TMJ movement was required for drinking. The data suggested that the decrease in body weight, food and water intake correlated with the development of TMJ arthritis.

In our morphological study, we also confirmed that the arthritic rats had several changes in TMJ. In a clinical case, marked fibrosis and degenerative cartilage were observed (Kobayashi et al., 2001). In the monoarthritic TMJ induced by CFA injection into the superior joint space of the rats, a very active chronic inflammation developed.

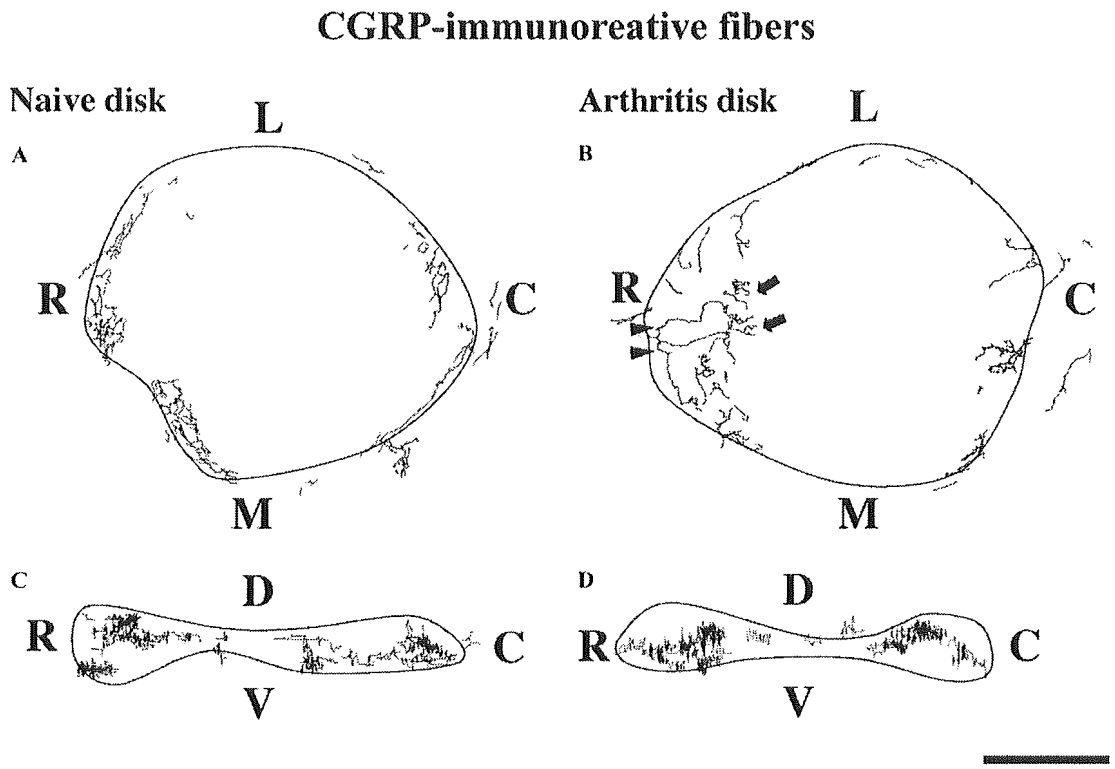

Fig. 7. Computer-aided, camera lucida drawing of CGRP immunoreactive fibers in the whole-mount preparation of the TMJ disk of naive rat (A,B) and arthritic rat (C,D). In the arthritic rats the proliferating fibers overlapped (arrowheads) and the nerve fibers never extended to the central part of the disk (arrows) similar to PGP-9.5 immunoreactive fibers. (A,C) Dorsal view. (B,D) Lateral view. R, rostral; C, caudal; D, dorsal; M, medial; V, ventral. Size scale bar, 1 mm.

In the synovial membrane in the ankle joint of CFA polyarthritic rat, mononuclear cells infiltrated significantly (Wu et al., 2000). A previous report confirmed that the synovial membrane in polyarthritic rat showed enhanced vascularization in the sublining layer in the rostro-caudal portion of the synovial membrane at 3 weeks after CFA injection but no progressive inflammatory findings such as synovial hypertrophy or inflammatory cell infiltration in TMJ (Nozawa-Inoue et al., 1998). Our results were rather similar, except that a few lymphatic cells or granular cells were scattered throughout the subintimal synovial tissue.

4.2. Innervations of TMJ and TMJ disk

The TMJ was innervated caudally by the auriculotemporal nerve, rostro-medially by the masseteric nerve, and rostro-laterally by the deep temporal nerve (Kobayashi et al., 1994). In the present study, we have macroscopically confirmed that the disk was also innervated by the same nerves.

Some investigators have examined the innervations of the TMJ by silver impregnation techniques (Dreessen et al., 1990; Johansson et al., 1986; Wink et al., 1992). Nerve distribution in the disk has been variously reported, presumably depending on the technique used. Current immunohistochemical studies have served to identify the peptidergic innervations in the TMJ disk and its surrounding soft tissues. We have focused on nerve fibers containing neuropeptides such as PGP-9.5 and CGRP in the joints using immunohistochemical methods. PGP-9.5 is a major protein component of the neuronal cytoplasm (Doran et al., 1983; Thompson et al., 1983), and is the most sensitive marker of nerve fibers (Dalsgaard et al., 1989; Gulbenkian et al., 1987; Maeda et al., 1994). CGRP is predominantly present in small and medium-size primary sensory neurons, and is a good marker of peripheral sensory nerve fibers (McCarthy and Lawson, 1990).

All of the innervations of the TMJ using antiserum to PGP-9.5 and CGRP in 18-day-old rat have been identified (Shimizu et al., 1996). Moreover, the distribution of CGRP ir fibers in the rat TMJ was investigated focusing in particular on the disk and synovial membrane by the whole-mount preparation method from the dorsal and ventral view (Kido et al., 1993). These reports provided a wealth of information on the nerve fibers in the TMJ, but the three-dimensional distribution and detailed innervation of the disk remain unclear. Nerve fibers were innervated toward the central part of the TMJ disk with complex meandering in the rostral and caudal parts, but with less meandering in the medial and

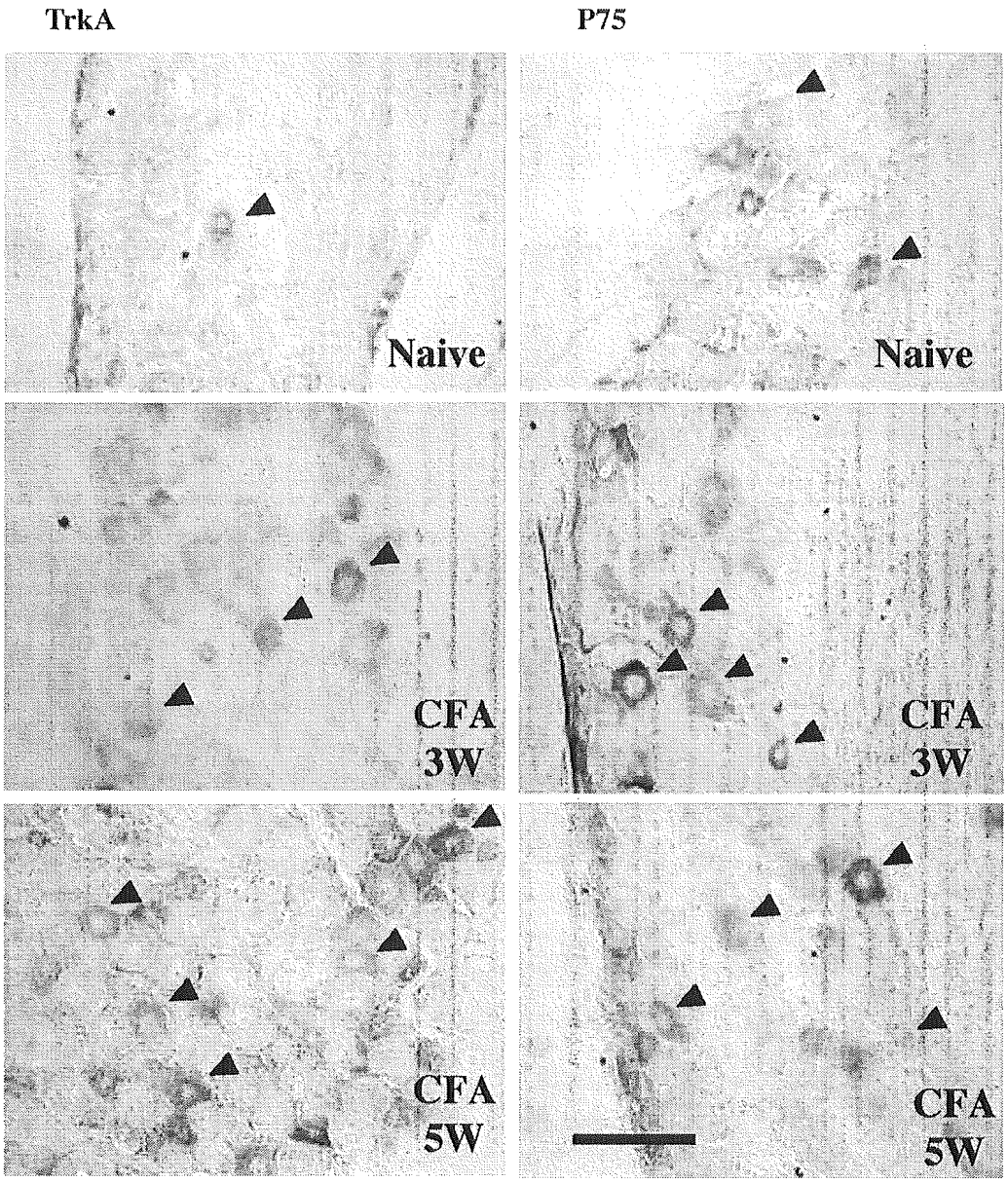

Fig. 8. Photomicrographs of TrkA (A,C,E) and P75 (B,D,F) immunopositive cells in the trigeminal ganglion in naive and CFA arthritic rats. (A,B) naive rats. (C,D) 3 weeks after CFA injection. (E,F) 5 weeks after CFA injection . Size scale bar, 100 μm.

lateral parts. The reason for the different nerve extension was suspected to be the variety of animal conditions in which the TMJ disk is forcefully expanded and contracted in the rostro-caudal direction by the movement of the TMJ. A dense innervation was observed in the rostral and caudal edges of the disk. The TMJ mainly moves in the rostro-caudal direction (Byrd and Chai, 1988). These innervation patterns may be important to receive sensory inputs to modulate the TMJ movement.

PGP-9.5 ir fibers were distributed more densely than CGRP ir fibers in the TMJ disk. This results suggested that PGP-9.5 positive- but CGRP negative-nerve fibers were innervating the TMJ disk. Previous studies indicated the existence of other peptidergic nerve fibers such as substance P (Kido et al., 1993), neuropeptide Y (Shimizu et al., 1996), tyrosine hydroxylase (Kido et al., 2001), and vasoactive intestinal polypeptide (Kido et al., 2001) in the TMJ disk. These fibers were suspected to be involved in metabolic function as well as nociception.

4.3. Increased innervation in TMJ disk

We studied innervation of TMJ disk 5 weeks after CFA. It was reported that substance P and CGRP extraction in the arthritic TMJ were increased 28 days after CFA injection (Carleson et al., 1997). Numerous

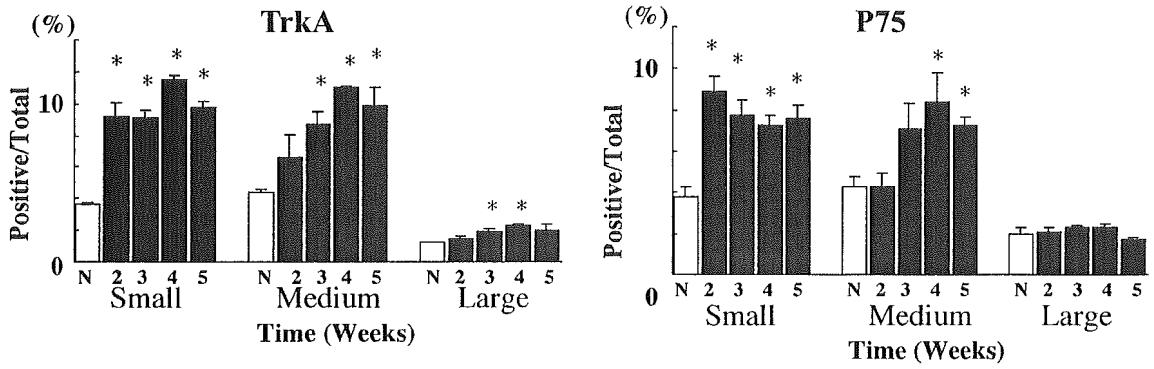

Fig. 9. Ratio of TrkA and P75 immunoreactive cells in the trigeminal ganglion. N, 2, 3, 4 and 5 indicated naive, 2, 3, 4 and 5 weeks after injection of CFA, respectively; small, medium, large indicate the cell diameter classified (<20, 20–30, > 30 μm) by cell diameter frequency distribution. ($n = 5$) *$P < 0.05$.

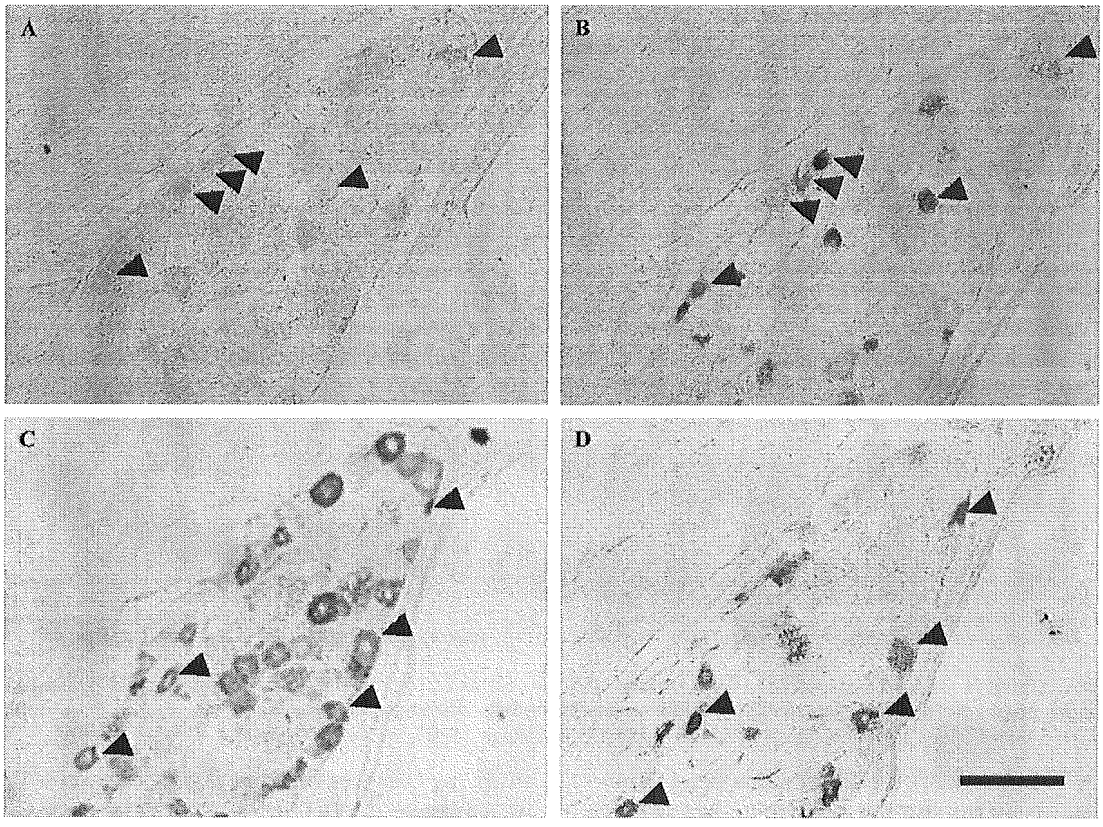

Fig. 10. Photomicrographs of trkA (A) and CGRP (B) or p75(C) and CGRP (D) immunopositive cells in the trigeminal ganglia at 5 weeks after CFA injection in serial section. The co-expressing cells indicated (arrowheads). Size scale bar, 100 μm.

CGRP or PGP-9.5 immunoreactive fibers were observed on day 21 in tarsal joints (Imai et al., 1997). Compared with the naive rats, the total length and length density of PGP-9.5 and CGRP ir fibers increased in the arthritic rats. Although each fiber plexus of the rostro-medial, rostro-lateral and caudal parts are located separately on the disk in naive rats, the proliferated fiber plexus in the rostro-medial part merged with the rostro-lateral part of the disk in the arthritic rats. Fiber plexus of caudal part did not seem to be affected by arthritis. Further experiments were needed to clarify regional difference of increased innervation.

Compared to naive rats, nerve fibers were distributed in the central part of the TMJ disk of arthritic rats, and

the sprouted fibers coursed toward the central part of the disk. This fact suggested the possibility that some trophic factors promoted the nerve extension.

We explored the possibility that neurotrophic factors may have been involved in this plastic change of the nerve fibers. The inflammatory cytokines such as interleukin-1 (Kopp, 1998; Nordahl et al., 2001), interleukin-6 (Kubota et al., 1998), interleukin-8 (Nanki et al., 2001), and tumor necrosis factor-α (Fu et al., 1995) increased in peripheral tissue following CFA injection. Interleukin-1 and tumor necrosis factor-α also contributed to the secretion of NGF in peripheral nervous systems (Bennett et al., 1998; Carman-Krzan et al., 1991; Hattori et al., 1993; Koltzenburg et al., 1999; Lindholm et al., 1987; Oddiah et al., 1998; Steiner et al., 1991). NGF promoted the sprouting of peripheral nerves (Albers et al., 1994; Kinkelin et al., 2000). CGRP ir fibers were shown to sprout in the peripheral tissue in inflammation (Weihe et al., 1988; Reinert et al., 1998). It was assumed that the sprouting occurred as a result of the infiltration of cytokines and neurotrophins in the peripheral tissue after inflammation such as TMJ arthritis.

The fibers sprouted toward the central part of the TMJ disk, and distributed on the surface of the disk in the arthritic rats. The trophic factor may intensively promote the sprouting of fibers on the surface of the disk. This factor supplied from synovial membrane may be kept in the synovial fluid contacting the disk. Inflammatory cells in the synovial membrane secreted NGF (Wu et al., 2000) and infiltrated the joint cavity with synovial fluid of arthritic rats. Previous studies reported that NGF increased in synovial fluid in arthritis (Aloe et al., 1992; Dicou et al., 1996; Falcini et al., 1996).

Neurotrophin-sensitized sensory neurons-induced hyperalgesia (Shu and Mendell, 1999), and NGF-induced hypersensitivity by the sprouting of peripheral nerves in peripheral tissue (Bennett et al., 1998; Donnerer et al., 1992a; Donnerer and Stein, 1992b; Leslie et al., 1995; Woolf et al., 1997). With TMJ arthritis in the CFA arthritic rats, sensitization and hyperalgesia of sensory neurons reflectively induced behavioral changes such as lower food and water intake.

4.4. Up-regulation of trkA and p75 in trigeminal ganglia of CFA arthritic rats

The proportion of neurons with p75 and trkA was rather low in the present study compared to data reported in the literature (Kashiba et al., 1995; McMahon et al., 1994). From observing the specimens to determine strictly immunopositive cells, when no clear decision could be made, we opted for negative. Any difference may be explained by the variety of spinal levels or rat species.

We showed that expression of trkA and p75 increased in small and medium trigeminal ganglia neurons from weeks 2 to 5 after CFA injection. However, there is no evidence that the increase in expression of trkA and p75 among trigeminal ganglia neurons was directly related to arthritis of the TMJ per se. But it is proper that up-regulation of trkA and p75 in trigeminal ganglia related to arthritis of the TMJ since all of the sensory nerves innervating TMJ disk was originated from trigeminal ganglia. These facts suggest that small and medium neurons may be sensitive to NGF and that the sprouting fibers are mostly thin. We confirmed that the trkA- or p75-positive cells in the trigeminal ganglion are also CGRP-positive, which suggests the possibility that the sprouting CGRP fibers in the TMJ disk originated from trkA- or p75-positive cells in the trigeminal ganglia.

Earlier studies showed that trkA could be up-regulated after exposure to NGF (Goodness et al., 1997; Holtzman et al., 1992). NGF increased in the synovial membrane and synovial fluid after CFA injection, and was retrogradely transported to dorsal root ganglia (DRGs) (Goedert et al., 1981). Our result supported that the NGF receptor, trkA and p75 expression increased in trigeminal ganglia reacting to the transported NGF. However, some investigators reported a decrease in p75 in L3-L5 DRGs after CFA injection (Pezet et al., 2001). This difference may be caused by the variety of joints, spinal levels or rat species. We indicated that CFA arthritis increased NGF receptors in the trigeminal ganglia and had the potential ability to extend nerve terminals in the TMJ disk.

Expression of trkA and p75 at the TMJ disk is still unclear. The presence of these receptors on the sprouting fibers should be investigated in future.

Acknowledgements

This study was partly supported by grants from the Ministry of Education, Culture, Sports, Science and Technology (Nos. 13470430 and 11470433).

References

Albers KM, Wright DE, Davis BM. Overexpression of nerve growth factor in epidermis of transgenic mice causes hypertrophy of the peripheral nervous system. J Neurosci 1994;14:1422–32.

Aloe L, Tuveri MA, Carcassi U, Levi-Montalcini R. Nerve growth factor in the synovial fluid of patients with chronic arthritis. Arthritis Rheum 1992;35:351–5.

Alstergren P, Kopp S. Pain and synovial fluid concentration of serotonin in arthritic temporomandibular joints. Pain 1997;72:137–43.

Appelgren A, Appelgren B, Kopp S, Lundeberg T, Theodorsson E. Substance P-associated increase of intra-articular temperature and pain threshold in the arthritic TMJ. J Orofac Pain 1998;12:101–7.

Barde YA. Trophic factors and neuronal survival. Neuron 1989;2:1525–34.

Bennett DL, Koltzenburg M, Priestley JV, Shelton DL, McMahon SB. Endogenous nerve growth factor regulates the sensitivity of nociceptors in the adult rat. Eur J Neurosci 1998;10:1282–91.

Byers MR, Schatteman GC, Bothwell M. Multiple functions for NGF receptor in developing, aging and injured rat teeth are suggested by epithelial, mesenchymal and neural immunoreactivity. Development 1990;109:461–71.

Byers MR, Wheeler EF, Bothwell M. Altered expression of NGF and P75 NGF-receptor by fibroblasts of injured teeth precedes sensory nerve sprouting. Growth Factors 1992;6:41–52.

Byrd KE, Chai Y. Three-dimensional movement analysis of lateral pterygoid electromyographic activity during mastication in the rat. Arch Oral Biol 1988;33:635–40.

Campenot RB. Local control of neurite sprouting in cultured sympathetic neurons by nerve growth factor. Brain Res 1987;465:293–301.

Carleson J, Bileviciute I, Theodorsson E, et al. Effects of adjuvant on neuropeptide-like immunoreactivity in the temporomandibular joint and trigeminal ganglia. J Orofac Pain 1997;11:195–9.

Carman-Krzan M, Vige X, Wise BC. Regulation by interleukin-1 of nerve growth factor secretion and nerve growth factor mRNA expression in rat primary astroglial cultures. J Neurochem 1991;56:636–43.

Dalsgaard CJ, Rydh M, Haegerstrand A. Cutaneous innervation in man visualized with protein gene product 9.5 (PGP-9.5) antibodies. Histochemistry 1989;92:385–90.

Dicou E, Perrot S, Menkes CJ, Masson C, Nerriere V. Nerve growth factor (NGF) autoantibodies and NGF in the synovial fluid: implications in spondylarthropathies. Autoimmunity 1996;24: 1–9.

Donnerer J, Schuligoi R, Stein C. Increased content and transport of substance P and calcitonin gene-related peptide in sensory nerves innervating inflamed tissue: evidence for a regulatory function of nerve growth factor in vivo. Neuroscience 1992a;49:693–8.

Donnerer J, Stein C. Evidence for an increase in the release of CGRP from sensory nerves during inflammation. Ann N Y Acad Sci 1992b;657:505–6.

Doran JF, Jackson P, Kynoch PA, Thompson RJ. Isolation of PGP-9.5, a new human neurone-specific protein detected by high-resolution two-dimensional electrophoresis. J Neurochem 1983;40:1542–7.

Dreessen D, Halata Z, Strasmann T. Sensory innervation of the temporomandibular joint in the mouse. Acta Anat 1990;139:154–60.

Dyck PJ, Peroutka S, Rask C, et al. Intradermal recombinant human nerve growth factor induces pressure allodynia and lowered heat-pain threshold in humans. Neurology 1997;48:501–5.

Falcini F, Matucci Cerinic M, Lombardi A, et al. Increased circulating nerve growth factor is directly correlated with disease activity in juvenile chronic arthritis. Ann Rheum Dis 1996;55:745–8.

Fu K, Ma X, Zhang Z, Chen W. Tumor necrosis factor in synovial fluid of patients with temporomandibular disorders. J Oral Maxillofac Surg 1995;53:424–6.

Fundin BT, Arvidsson J, Rice FL. Innervation of nonmyatacial vibrissae in the rat. J Comp Neurol 1995;357:501–12.

Goedert M, Stoeckel K, Otten U. Biological importance of the retrograde axonal transport of nerve growth factor in sensory neurons. Proc Natl Acad Sci USA 1981;78:5895–8.

Goodness TP, Albers KM, Davis FE, Davis BM. Overexpression of nerve growth factor in skin increases sensory neuron size and modulates Trk receptor expression. Eur J Neurosci 1997;9:1574–85.

Gulbenkian S, Wharton J, Polak JM. The visualization of cardiovascular innervations in the guinea pig using an antiserum to protein gene product 9.5 (PGP-9.5). J Auton Nerv Syst 1987;18:235–47.

Hattori A, Tanaka E, Murase K, et al. Tumor necrosis factor stimulates the synthesis and secretion of biologically active nerve growth factor in non-neuronal cells. J Biol Chem 1993;268:2577–82.

Holtzman DM, Li Y, Parada LF, et al. p140trk mRNA marks NGF-responsive forebrain neurons: evidence that trk gene expression is induced by NGF. Neuron 1992;9:465–78.

Imai S, Tokunaga Y, Konttinen YT, Maeda T, Hukuda S, Santavirta S. Ultrastructure of the synovial sensory peptidergic fibers is distinctively altered in different phases of adjuvant-induced arthritis in rats: ultramorphological characterization combined with morphometric and immunohistochemical study for substance P, calcitonin gene-related peptide, and protein gene product 9.5. J Rheumatol 1997;24:2177–87.

Johansson A, Isacsson G, Isberg A, Grandholm A. Distribution of substance P-like immunoreactive nerve fibers in temporomandibular joint soft tissue of the monkey. Second J Dent Res 1986;94:225–30.

Kapila S, Lee C, Tavakkoli Jou MR, Miller AJ, Richards DW. Development and histologic characterizations of an animal model of antigen-induced arthritis of the juvenile rabbit temporomandibular joint. J Dent Res 1995;74:1870–9.

Kapila S, Xie Y. Targeted induction of collagenase and stromelysin by relaxin in unprimed and beta-estradiol-primed diarthrodial joint fibrocartilaginous cells but not in synoviocytes. Lab Invest 1998;78:925–38.

Kashiba H, Noguchi K, Ueda Y, Senba E. Coexpression of trk family members and low-affinity neurotrophin receptors in rat dorsal root ganglion neurons. Brain Res Mol Brain Res 1995;30:158–64.

Keller JH, Moffett Jr BC. Nerve endings in the temporomandibular joint of the rhesus mascaque. Anat Rec 1968;160:587–94.

Kido MA, Kiyoshima T, Kondo T, et al. Distribution of substance P and calcitonin gene-related peptide-like immunoreactive nerve fibers in the rat temporomandibular joint. J Dent Res 1993;72:592–8.

Kido MA, Zhang JQ, Muroya H, Yamaza T, Terada Y, Tanaka T. Topography and distribution of sympathetic nerve fibers in the rat temporomandibular joint: immunocytochemistry and ultrastructure. Anat Embryol (Berl) 2001;203:357–66.

Kinkelin I, Motzing S, Koltenzenburg M, Brocker EB. Increase in NGF content and nerve fiber sprouting in human allergic contact eczema. Cell Tissue Res 2000;302:31–7.

Kobayashi R, Utsunomiya T, Yamamoto H, Nagura H. Ankylosis of the temporomandibular joint caused by rheumatoid arthritis: a pathological study and review. J Oral Sci 2001;43:97–101.

Kobayashi T, Ohashi Y, Maeda T, Takano Y. Innervation of Rat Temporomandibular joint – An immunohistochemical study using protein gene product 9.5 antibody. J Jpn Stomatol Soc 1994;43:369–85 (Japanese).

Koltzenburg M, Bennett DL, Shelton DL, McMahon SB. Neutralization of endogenous NGF prevents the sensitization of nociceptors supplying inflamed skin. Eur J Neurosci 1999;11:1698–704.

Kopp S. The influence of neuropeptides, serotonin, and interleukin 1beta on temporomandibular joint pain and inflammation. J Oral Maxillofac Surg 1998;56:189–91.

Kubota E, Kubota T, Matsumoto J, Shibata T, Murakami KI. Synovial fluid cytokines and proteinases as markers of temporomandibular joint disease. J Oral Maxillofac Surg 1998;56:192–8.

Lee Y, Kawai Y, Shiosaka S, et al. Coexistence of calcitonin gene-related peptide and substance P-like peptide in single cells of the trigeminal ganglion of the rat: immunohistochemical analysis. Brain Res 1985;330:194–6.

Leslie TA, Emson PC, Dowd PM, Woolf CJ. Nerve growth factor contributes to the up-regulation of growth-associated protein 43 and preprotachykinin A messenger RNAs in primary sensory neurons following peripheral inflammation. Neuroscience 1995;67:753–61.

Lindholm D, Heumann R, Meyer M, Thoenen H. Interleukin-1 regulates synthesis of nerve growth factor in non-neuronal cells of rat sciatic nerve. Nature 1987;330:658–9.

Maeda T, Sodeyama T, Hara K, Takano Y. Evidence for the existence of intraepithelial nerve endings in the junctional epithelium of rat molars: an immunohistochemical study using protein gene product 9.5 (PGP-9.5) antibody. J Periodontal Res 1994;29:377–85.

McCarthy PW, Lawson SN. Cell type and conduction velocity of rat primary sensory neurons with calcitonin gene-related peptide-like immunoreactivity. Neuroscience 1990;34:623–32.

McMahon SB, Armanini MP, Ling LH, Phillips HS. Expression and coexpression of Trk receptors in subpopulations of adult primary sensory neurons projecting to identified peripheral targets. Neuron 1994;12:1161–71.

Murakami K, Segami N, Fujimura K, Iizuka T. Correlation between pain and synovitis in patients with internal derangement of the temporomandibular joint. J Oral Maxillofac Surg 1991;49:1159–61.

Nanki T, Nagasaka K, Hayashida K, Saita Y, Miyasaka N. Chemokines regulate IL-6 and IL-8 production by fibroblast-like synoviocytes from patients with rheumatoid arthritis. J Immunol 2001;167:5381–5.

Nordahl S, Alstergren P, Eliasson S, Kopp S. Radiographic signs of bone destruction in the arthritic temporomandibular joint with special reference to markers of disease activity. A longitudinal study. Rheumatology 2001;40:691–4.

Nozawa-Inoue K, Takagi R, Kobayashi T, Ohashi Y, Maeda T. Immunocytochemical demonstration of the synovial membrane in experimentally induced arthritis of the rat temporomandibular joint. Arch Histol Cytol 1998;61:451–66.

Oddiah D, Anand P, McMahon SB, Rattray M. Rapid increase of NGF, BDNF and NT-3 mRNAs in inflamed bladder. Neuroreport 1998;9:1455–8.

Pezet S, Onteniente B, Jullien J, et al. Differential regulation of NGF receptors in primary sensory neurons by adjuvant-induced arthritis in the rat. Pain 2001;90:113–25.

Reinert A, Kaske A, Mense S. Inflammation-induced increase in the density of neuropeptide-immunoreactive nerve endings in rat skeletal muscle. Exp Brain Res 1998;121:174–80.

Shimizu S, Kido MA, Kiyoshima T, Tanaka T. Postnatal development of protein gene-related peptide-like immunoreactive nerve fivers in the rat temporomandibular joint. Anat Rec 1996;245:568–76.

Shu XQ, Mendell LM. Neurotrophins and hyperalgesia. Proc Natl Acad Sci USA 1999;96:7693–6.

Steiner P, Pfeilschifter J, Boeckh C, Radeke H, Otten U. Interleukin-1 beta and tumor necrosis factor-alpha synergistically stimulate nerve growth factor synthesis in rat mesangial cells. Am J Physiol 1991;261:792–8.

Swift JQ, Roszkowski MT, Alton T, Hargreaves KM. Effect of intra-articular versus systemic anti-inflammatory drugs in a rabbit model of temporomandibular joint inflammation. J Oral Maxillofac Surg 1998;56:1288–96.

Thompson RJ, Doran JF, Jackson P, Dhillon AP, Rode J. PGP-9.5 a new marker for vertebrate neurons and neuroendocrine cells. Brain Res 1983;278:224–8.

Weihe E, Nohr D, Millan MJ, et al. Peptide neuroanatomy of adjuvant-induced arthritic inflammation in rat. Agents Actions 1988;25:255–9.

Wheeler EF, Bothwell M. Spatiotemporal patterns of expression of NGF and the low-affinity NGF receptor in rat embryos suggest functional roles in tissue morphogenesis and myogenesis. J Neurosci 1992;12:930–45.

Wheeler EF, Naftel JP, Pan M, von Bartheld CS, Byers MR. Neurotrophin receptor expression is induced in a subpopulation of trigeminal neurons that label by retrograde transport of NGF or fluoro-gold following tooth injury. Brain Res Mol Brain Res 1998;61:23–38.

Wink CS, St Onge M, Zimny ML. Neural elements in the human temporomandibular articular disc. J Oral Maxillofac Surg 1992;50:334–7.

Woolf CJ, Allchorne A, Safieh-Garabedian B, Poole S. Cytokines, nerve growth factor and inflammatory hyperalgesia: the contribution of tumour necrosis factor alpha. Br J Pharmacol 1997;121:417–24.

Wu Z, Nagata K, Iijima T. Immunohistochemical study of NGF and its receptors in the synovial membrane of the ankle joint of adjuvant-induced arthritic rats. Histochem Cell Biol 2000;114:453–9.

Zimmermann M. Ethical guidelines for investigation of experimental pain in conscious animals. Pain 1983;16:109–10.

THE JOURNAL OF COMPARATIVE NEUROLOGY 461:140–150 (2003)

Central Projection of Unmyelinated (C) Primary Afferent Fibers from Gastrocnemius Muscle in the Guinea Pig

LI-JUN LING,[1,2] TAKASHI HONDA,[3] YASUHIRO SHIMADA,[2] NORIYUKI OZAKI,[1] YOUSUKE SHIRAISHI,[1] AND YASUO SUGIURA[1]*

[1]Department of Functional Anatomy and Neuroscience, Nagoya University Graduate School of Medicine, Nagoya 466-8550, Japan

[2]Department of Anesthesiology, Nagoya University Graduate School of Medicine, Nagoya 466-8550, Japan

[3]Department of Anatomy, Fukushima Medical College, Fukushima 960-1295, Japan

ABSTRACT

We have demonstrated the central projections of muscle C or group IV afferent fibers in the guinea pig by tracing arborizations in the spinal cord. C afferent fibers from the gastrocnemius muscle (GCM) were electrophysiologically identified by conduction velocity (less than 1 m/second). A single neuron in the lumbar 5 dorsal root ganglion (L5 DRG) was intracellularly labeled with *Phaseolus vulgaris* leucoagglutinin (PHA-L). After iontophoretic injection of PHA-L, we processed the lumbar cord and L5 DRG for PHA-L immunohistochemistry. Six muscle C afferent fibers from 40 animals were labeled, and whole trajectories were recovered. Labeled fibers were reconstructed by tracing of the arbor in serial parasagittal sections. The GCM C afferents projected rostrocaudally for two or three segments and ran at the surface of the dorsal funiculus, giving off collaterals into laminae I and II and sometimes into parts of lamina III. We determined, based on the branching pattern and form of the terminal plexus, that the branching of muscle C afferent fibers showed an intermediate pattern that fell morphologically between the terminal patterns of somatic and visceral afferents. The numbers and sizes of fiber swellings and terminal swellings were measured on all collateral branches. We found that the area of distribution of the terminal swellings of muscle C afferent fibers is larger than that of somatic terminals but that the density of terminal swellings in the terminal area was lower than that of the somatic terminals. J. Comp. Neurol. 461:140–150, 2003.

Indexing terms: group IV afferent fiber; muscle; spinal termination; intracellular labeling; PHA-L

The spinal terminations of fine afferent fibers from muscle mediate mechanical sensation, including perceptions of local pressure and pain. Thinly myelinated (group III) and unmyelinated (C and group IV) fibers are known to be major components of muscle afferent fibers (Mense, 1993). A few reports have dealt with central terminals of C afferent fibers from muscles, but anatomical information in this regard is still fragmentary (Ygge, 1989; Hirakawa et al., 1992; Torre et al., 1995).

The distribution of central terminations of afferent fibers has previously been demonstrated using horseradish peroxidase (HRP) or wheat germ agglutinin (WGA)-HRP, either injected directly or applied to the identified organs or muscles (Light and Perl, 1979a; Carson and Mesulam, 1982; Craig and Mense, 1983; Ygge and Grant, 1983; Abraham et al., 1984; Cervero and Connell, 1984; Pfaller and Arvidsson, 1988; Capra and Wax, 1989; Arvidsson and Pfaller, 1990; Arvidsson and Rice, 1991; Castro-Lopes and Coimbra, 1991; Prihoda et al., 1991). Abraham and Swett (1986) reported that neck and forelimb muscle af-

Grant sponsor: Japanese Ministry of Education, Culture, Sports, Science and Technology.

*Correspondence to: Yasuo Sugiura, Department of Functional Anatomy and Neuroscience, Nagoya University Graduate School of Medicine, 65 Tsurumaicho, Showaku, Nagoya 466-8550, Japan.
E-mail: ysugiura@med.nagoya-u.ac.jp

Received 15 July 2002; Revised 13 September 2002; Accepted 18 December 2002

DOI 10.1002/cne.10619

Published online the week of May 5, 2003 in Wiley InterScience (www.interscience.wiley.com).

ferents terminated in laminae I and V. However, different results have been obtained from labeling gastrocnemius (GC)-soleus muscle; Brushart et al. (1981) demonstrated dense projections terminating in substantia gelatinosa, whereas Kalia et al. (1981) showed diffuse projections terminating in laminae I–V. Other studies showed that GC muscle fibers terminated in laminae I and V but not in lamina II (Mense and Craig, 1988). These conflicting results, however, are due to the different transport characteristics of HRP and WGA-HRP and the differences in the species and GC muscles studied.

In other studies, single primary afferent fibers from skin and muscles were labeled with HRP that had been injected in the dorsal funiculus in order to demonstrate different morphological features of terminal collaterals in the spinal cord (Snow et al., 1976; Brown et al., 1978, 1980, 1991; Light and Perl, 1979b; Ishizuka et al., 1979; Brown, 1981; Gobel et al., 1981; Réthelyi et al., 1982; Fyffe, 1984; Mense and Prabhakar, 1986; Hongo et al., 1987). The intraaxonal labeling with HRP demonstrated that the projections of fibers originating in muscle or other deep tissue terminated in lamina I only or in laminae I, IV, and V (Mense et al., 1981; Hoheisel et al., 1989). By contrast, the nonproprioceptive receptors of deep tissues terminated in laminae II and IV–VI. This differential termination pattern (myelinated vs. unmyelinated) may reflect a variation of receptor modality or different types of afferent fibers. In fact, in guinea pigs, unmyelinated (C) fibers whose receptive fields are located in skin and toe terminated mainly in laminae I and II of the cervical, thoracic, and lumbar cord (Sugiura et al., 1986, 1989). Similarly, Alvarez et al. (1993) noticed that central terminations of C fibers in monkey skin also located to laminae I and II. On the other hand, visceral C afferent branches in guinea pigs terminated in laminae I, V, and X (Sugiura et al., 1989, 1993).

Electrophysiological recordings of dorsal root ganglion neurons and iontophoretic injection with *Phaseolus vulgaris* leucoagglutinin (PHA-L; Gerfen and Sawchenko, 1984; TerHorst et al., 1985) into cell bodies demonstrated terminal arbors of several kinds of unmyelinated C-fibers from skin and viscera (Sugiura et al., 1986, 1989, 1993). However, whole trajectories into the spinal cord of C or group IV afferent fibers from muscle have not been demonstrated. Here, we sought to elucidate the entire arborization of central terminals of unmyelinated C fibers from lateral gastrocnemius (LGC) muscle in guinea pigs.

MATERIALS AND METHODS

Animals and surgical techniques

The experiments were carried out under the control of the local animal ethics committee in accordance with The Guidelines for Animal Experiments in Nagoya University Graduate School of Medicine (No. 13030) and the Animal Protection and Management Law of the Japanese Government (No. 105). The experiments were performed on 40 female guinea pigs, each weighing from 200 to 300 g. While an animal was deeply anesthetized with sodium pentobarbital (50 mg/kg, ip), we inserted a cannula into the trachea and a catheter into the external jugular vein under surgically clean conditions. After we administered the paralytic suxamethonium chloride (0.4 mg/hour, iv), we maintained respiration by means of a positive-pressure

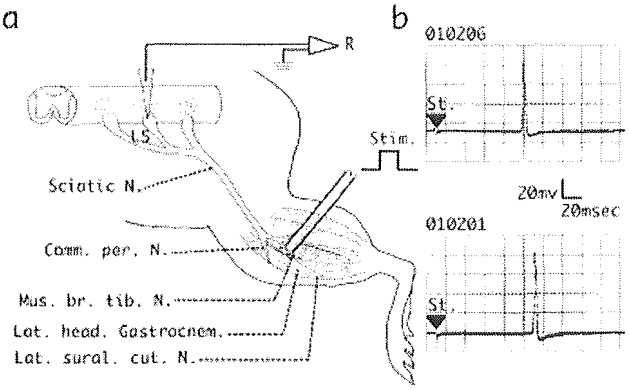

Fig. 1. **a:** The intracellular recording setup. A micropipette was inserted in an L5 DRG (L5) cell for intracellular recording and iontophoretic injection with the PHA-L solution. Stim, electric stimulation; Comm. per N., common peroneal nerve; Mus. br. tib. N., muscle branch of tibial nerve; Lat, lateral; Gastrocnem, gastrocnemius; cut, cutaneous. **b:** Action potentials of the intracellular recording in the L5 DRG cell. St, electric stimulation; 5-mA stimulation evoked about 80-mV action potentials with a 100-msec duration at −60-mV resting potential in unit No. 010201 and a 90-msec latency at −50-mV resting potential in unit No. 010206.

pump; additional doses of sodium pentobarbital and suxamethonium chloride were given as necessary. Heart rate was monitored throughout the experiment. During the experiment and anesthetic-recovery period, we maintained the body temperature at 38°C ± 1°C by means of a heating pad. After securing the animal in a prone position within a stereotaxic frame, we prepared the LGC muscle and muscular branches of the tibial nerve for stimulation and the lumbar 5 (L5) DRG for recording using a microelectrode amplifier (Nihon-Kohden MEZ-8201) as shown in Figure 1a. Fine glass micropipettes filled with a 2.5% solution of PHA-L dissolved in 0.1 M KCl were used to record the neuronal activity from DRG cell bodies.

After we stimulated the LGC muscle branch of the tibial nerve with an electrical pulse (0.05–0.1 msec) above C fiber threshold (6–10 V or 5 mA), we recorded the responses of cell bodies in the L5 DRG (Fig. 1b). We calculated both the conduction velocity from the recorded response latency and the conduction distance (40–50 mm) between the stimulation electrode (LGC muscle branch) and the L5 DRG neuron. In this study, the conduction velocities of unmyelinated C fibers were less than 1 m/second. After confirmation of action potentials with C fiber latency, we applied PHA-L intracellularly by positive iontophoretic current (5×10^{-9} A) for 5 minutes or more (Sugiura et al., 1986). Only one neuron was intracellularly labeled in each animal. At the end of the electrophysiological experiment, the wounds of animals were closed by standard surgical techniques, and antibiotics were topically administered. Animals were kept under optimal recovery conditions for 3–5 days afterward. As a final experiment, animals deeply anesthetized with sodium pentobarbital (50 mg/kg, ip) were perfused transcardially with a fixative containing 2% paraformaldehyde and 10% saturated picric acid in 0.1 M phosphate buffer (pH 7.4). After perfusion, the lumbar enlargement and the injected L5 DRG were removed and placed in the same fixative overnight. All tissue blocks were processed after cryopro-

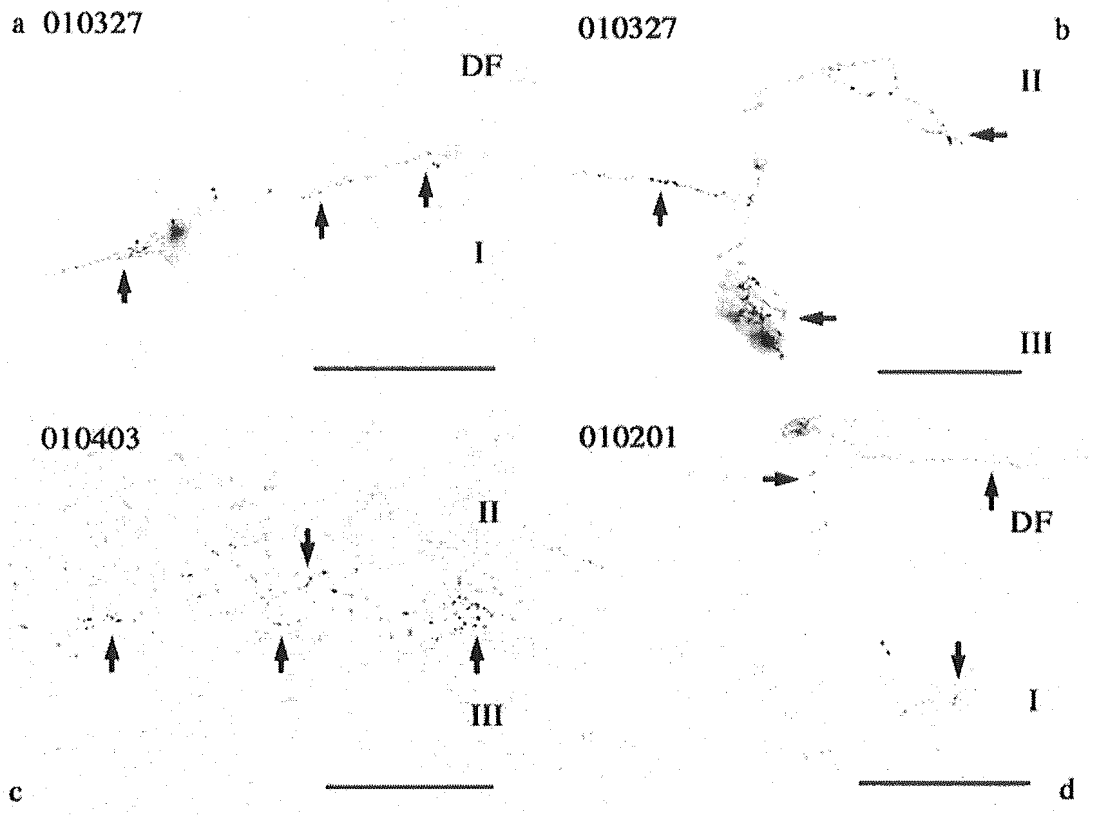

Fig. 2. Photomicrographs showing labeled fibers and terminal swellings. Arrows indicate labeled fiber or terminals. **a:** Terminals between dorsal funiculus (DF) and lamina I. **b:** Terminals between laminae II and III, which showed complicated, short terminal branches. **c:** Faintly stained terminals between laminae II and III, covering a terminal field of 300–400 μm. **d:** Collaterals given off from the main branch running on the surface of the DF. Terminal field was formed at the border between DF and lamina I. Scale bars = 100 μm.

tection in 20% sucrose and frozen in O.C.T. compound (Tissue Tek Sakura, Tokyo, Japan).

Immunohistochemistry

The L5 DRG was cut on a cryostat at 20 μm, and L1–L6 spinal segments were sectioned serially at 50 μm in the parasagittal plane on a freezing microtome. All tissue sections were processed for PHA-L immunohistochemistry. Tissue sections were immersed in a goat anti-PHA-L solution (1:1,000; Vector, Burlingame, CA) for 3 days. After rinses with phosphate-buffered saline (PBS; 0.1 M), sections were incubated with a biotinylated rabbit anti-goat IgG solution (1:200; Vector) for 2 hours, then incubated in a solution containing avidin and biotin-peroxidase complex (ABC; 1:200) at room temperature for 90 minutes. To visualize the presence of the PHA-L antibody, we immersed the sections in a solution of 0.1% 3-3′-diaminobenzidine tetrahydrochloride (DAB; Sigma, St. Louis, MO) with 0.023% hydrogen peroxide.

Analysis of results

Composite camera lucida drawings were made of the arbors of each labeled central process in the spinal cord as found in each parasagittal section. Three-dimensional reconstructions of fiber projections were also produced by tracing the arbors in individual sections and then combining them in a composite (Réthelyi and Capowski, 1977). The numbers and sizes of the terminal boutons on recovered central projections were measured on all collateral branches in each lamina.

RESULTS

Muscle C fibers or group IV fibers were identified in 40 female guinea pigs by the latency of the unitary response after electric stimulation of the LGC muscle branch of the tibial nerve (Fig. 1a). In the present study, unitary responses of all C fibers showed 80–100 msec latency (Fig. 1b). The conduction distance from the electric stimulation site to the L5 DRG was 40–50 mm. Mean conduction velocity of the muscle C fiber units was approximately 0.5 m/second. After confirmation of the intracellular recording, we attempted to identify the sensory modality. However, we could not find any responses elicited by natural stimuli (touch or pinch by forceps) from the skin, muscle, tendon, or deep connective tissues, nor any spontaneous response relating to the input of muscle tonus.

We then recovered the central terminal projections of six C fibers arising from the 40 labeled C afferent neurons. No labeled DRG cells could be found after PHA-L immunohistochemistry.